[redacted]

NASA TECHNICAL MEMORANDUM

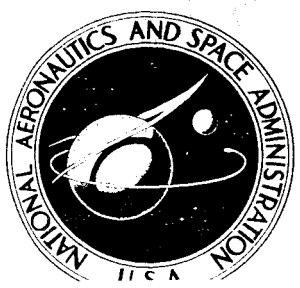

UB
NASA TM X-1178

[redacted]

PROJECT FIRE FLIGHT 1 HEATING AND PRESSURE MEASUREMENTS ON THE REENTRY-VEHICLE AFTERBODY AT A VELOCITY OF 38 000 FEET PER SECOND

by Travis H. Slocumb, Jr.

Langley Research Center
Langley Station, Hampton, Va.

NATIONAL AERONAUTICS AND SPACE ADMINISTRATION - WASHINGTON, D. C. - NOVEMBER 1965

[redacted]

[redacted]

NASA TM X-1178

PROJECT FIRE FLIGHT 1 HEATING AND PRESSURE MEASUREMENTS ON THE REENTRY-VEHICLE AFTERBODY AT A VELOCITY OF 38 000 FEET PER SECOND

By Travis H. Slocumb, Jr.

Langley Research Center
Langley Station, Hampton, Va.

[redacted]

NATIONAL AERONAUTICS AND SPACE ADMINISTRATION

[redacted]

PROJECT FIRE FLIGHT 1 HEATING AND PRESSURE MEASUREMENTS ON THE REENTRY-VEHICLE AFTERBODY AT A VELOCITY OF 38 000 FEET PER SECOND*

By Travis H. Slocumb, Jr.
Langley Research Center

SUMMARY

10305

The first of two scheduled Project Fire flights has been successfully flown to obtain measurements of reentry heating on a large-scale blunt body at hyperbolic velocity. The Fire 1 spacecraft was boosted by an Atlas D launch vehicle into a ballistic trajectory along the Eastern Test Range. The flight terminated with impact of the payload near Ascension Island. Prior to reentry into the sensible atmosphere, the reentry vehicle was accelerated to a velocity of 37 970 fps at a flight-path angle of -14.5° by a solid-propellant rocket motor which formed part of the Fire spacecraft. This report presents the results of heating and pressure experiments on the reentry-vehicle afterbody. In general, the pressures and total heating rates measured on the vehicle afterbody compared favorably with available wind-tunnel data and theoretical calculations.

INTRODUCTION

The rapid advancement of manned space exploration has accelerated the need for definition of the reentry heating environment at velocities exceeding the earth's escape velocity. These conditions would be representative of the heating environment experienced by vehicles returning from lunar or planetary missions. Thus, Project Fire was undertaken to provide large-scale, real-environment, reentry heating data at a velocity in excess of 37 000 fps which could be used to check the many available theoretical predictions and ground-facility results, and their extrapolations.

The primary objective of Project Fire was to obtain in-flight measurements of gas radiation and total heating on the forebody and afterbody of an Apollo-shaped vehicle. In addition, limited measurements of afterbody pressures and radio signal attenuation were planned. This report presents the results of the afterbody heating and pressure experiments for the first of two scheduled flights. Reference 1 presents an abbreviated version of all Project Fire Flight 1 results. Comprehensive data on the forebody total-heating experiment are given in reference 2.

SYMBOLS

c_p	specific heat of gold, Btu/lbm-^oR
D	diameter, in.
h	altitude, ft
l	distance along center line from forward shoulder to theoretical apex of conical afterbody, in. (see fig. 3)
M	Mach number
m	mass of gold calorimeters, lbm
p	pressure, psia
$\dot{q}$	heat-transfer rate, Btu/ft^2-sec
R	radius, in.
N_{Re}	Reynolds number (based on maximum diameter of reentry package)
S	exposed calorimeter surface area, ft^2
s	surface distance on reentry package measured from geometric stagnation point, in. (see fig. 3)
T	temperature, ^oR
t	time, sec
V	velocity, fps
x	distance along center line measured from forward shoulder on afterbody, in. (see fig. 3)
α	angle of attack, deg
α_{be}	absorptivity of beryllium
α_n	absorptivity of nichrome surface film on gold calorimeter
ϵ_n	emissivity of nichrome surface film on gold calorimeter
Γ	flight-path angle, deg
γ	isentropic exponent

ϕ circumferential location, deg (see fig. 3)

σ Stefan-Boltzmann constant

Subscripts:

a afterbody

av average

c corner

con convective

calc calculated

m pertaining to maximum cross-sectional dimensions

n nose

rad radiative

t stagnation

sp sonic point

tot total

∞ free stream

DESCRIPTION OF EXPERIMENT

Space Vehicle

The Project Fire space vehicle consisted of a powered spacecraft adapted to an Atlas D launch vehicle as shown in the schematic drawing of figure 1. Two systems were combined to form the powered spacecraft and these are termed the velocity package and reentry package. The velocity-package system included an Antares II-A5 solid rocket motor with a forward adapter and a supporting shell attached to the base of the motor. The velocity-package system was designed to accelerate the reentry package to a velocity in excess of escape velocity prior to reentry into the sensible atmosphere. The reentry package was mated to the front of the velocity package and contained the data-gathering instrumentation and associated equipment. The reentry package and Antares motor were protected from the launch environment by an aerodynamic shroud.

Reentry Package and Afterbody Experiments

The Project Fire reentry package is shown in the photograph of figure 2, and the pertinent geometry is presented in the schematic drawing of figure 3. The reentry package had a shape similar to that of the Project Apollo reentry vehicle and was primarily designed to measure radiative and total heating on both the blunt forebody and conical afterbody. As shown in figure 3, the reentry-package forebody consists of a layer-cake construction with three beryllium calorimeters sandwiched with protective layers of phenolic-asbestos. As each thin beryllium calorimeter was consumed by the severe heating during reentry into the earth's atmosphere, the succeeding phenolic-asbestos layer was timed to eject, and thus another cool and clean calorimeter was exposed. The ejections of the phenolic-asbestos shields were timed to provide calorimeter measurements during the initial part of the reentry heat pulse, at approximately peak heating, and midway on the decreasing side of the heat pulse. As previously mentioned, the forebody total-heating experiments are discussed in reference 2, whereas this report is concerned only with the afterbody experiments.

The conical afterbody of the reentry package basically was composed of a phenolic-asbestos sheet bonded to an aluminum-alloy shell. The phenolic-asbestos was coated with a layer of material composed of 75-percent silicon elastomer and 25-percent high-silica microballoons by weight to protect the afterbody from moisture penetration prior to launch, which could affect the telemetry antenna performance adversely. The afterbody of the reentry package was instrumented with gold-slug calorimeters to measure the afterbody heating rates at 12 locations; the pressure was measured at two locations and the total radiative flux at one position. These data were continuously measured and commutated at five samples per second. In addition to the other instrumentation, a telemetry antenna was embedded in the afterbody, and a C-band beacon antenna was positioned at the apex of the conical afterbody. The physical locations of the afterbody sensors are shown in figure 3, and dimensional locations are presented in table I. The afterbody instrumentation used to measure the data presented herein is discussed in the following sections.

Pressure sensors.- Two thermopile vacuum gages were used to measure the afterbody pressures. These sensors were sized to operate in a range up to 10 mm Hg with an accuracy, including that of the sensors and telemetry system, of approximately ±20 percent of the recorded value. The measured pressures corresponding to each pressure sensor were commutated at five samples per second.

Gold calorimeters.- The design details of the gold calorimeters are shown in the schematic drawing of figure 4, and the mass of each calorimeter is given in table II. The small gold slugs used as calorimeters were made thin (approximately 0.12 inch thick) to minimize the temperature gradient between front and rear surfaces. Each gold slug was coated with a 5-mil surface film of oxidized nichrome to increase the emissivity and, consequently, to increase the life of the calorimeters. The nichrome oxide surface film was applied to the gold slugs by flame spraying nichrome powder (80-percent nickel, 20-percent chrome) on the surface, vacuum heattreating for 3 hours at 1550° R and then allowing oxidation in air for 3 hours at 1550° R. The gold slugs were embedded in an

aluminum silicate housing which provided the insulation to isolate them from conduction effects of surrounding materials. Two thermocouples were attached to the rear surface of each calorimeter to record the temperature changes. The diffusion time through the calorimeters was less than 1/10 second, and therefore, within the $\pm 50^{\circ}$ R measuring accuracy of the thermocouples operating in conjunction with the telemetry system.

Trajectory and Sequence of Events

On April 14, 1964, at 21:42:25.536 Greenwich mean time, the Fire 1 space vehicle was launched from Cape Kennedy, Florida, along the Eastern Test Range toward Ascension Island. A schematic drawing of the flight trajectory and the associated sequence of events is presented in figure 5. In addition, as an aid in evaluating the measured afterbody data, curves of velocity, altitude, Mach number, and flight-path angle are presented in figure 6 for the reentry portion of the trajectory.

From a trajectory and sequence-of-events standpoint, Fire 1 was judged a complete success, since the vehicle performance and timed events were well within the prescribed limits. However, a faulty telemetry antenna and unexpected large coning motions impaired the reentry data to some degree. The reentry-package coning motions and the effect of these coning motions and telemetry dropout on the afterbody data will be discussed in subsequent sections of this report. More data on these two problems as well as more detailed information on the Fire 1 trajectory, sequence of events, and space vehicle can be found in reference 3.

Reentry-Package Motions

A brief discussion of the reentry-package motions during reentry is in order, since they directly affect the afterbody measurements. After separation from the Antares motor the reentry package maintained a coning angle of approximately 2° until 1665.94 seconds after launch. At this time the onboard yaw rate gyro indicated an abrupt, large increase in yaw rate which corresponded to a maximum total angle of attack of approximately 33°. Reentry films, ground tests, and calculations seemed to indicate that the sudden onset of body motions was caused by the spent Antares motor case passing in close proximity to the reentry package and disrupting the flow field. From an analysis of the body motions during time periods where there was sufficient data, the variation of total angle of attack with time from launch was obtained and presented in figure 7. The data indicate high initial total angles of attack which damped to approximately 13° as the region of maximum dynamic pressure was approached.

RESULTS AND DISCUSSION

Afterbody Pressures

The pressures measured at two locations on the afterbody of the Fire 1 reentry package (see fig. 3) are listed in table III and plotted in figure 8. These data are plotted as a function of time from launch in both dimensional

form and nondimensional form. The values of p_t were calculated for the Fire 1 trajectory by using an iterative solution of the pertinent equations presented in reference 4 in conjunction with the gas tables of reference 5.

The dimensional data in figure 8 indicated an initial pressure rise with a disturbance occurring at approximately 1665 seconds. In this region the variation of the data increased significantly because of the onset of severe reentry-package oscillations resulting in initial total angles of attack of 33°. The obvious lack of data between 1668 seconds and 1686 seconds was due partially to intermittent telemetry dropout and partially to the fact that the pressures exceeded the range of the sensors during this phase of the trajectory. Immediately following this period pressures were again within the sensible range of the instrumentation, and the data exhibit a reduction in scatter which was due to aerodynamic damping of the reentry package to total angles of attack of 13° or less.

It is customary to present afterbody pressures on blunt vehicles in the form of the ratio of the afterbody pressure to the stagnation pressure. The Fire 1 data are presented in this manner in figure 8 and compared with wind-tunnel data from references 6 and 7 on a Mach number basis. In the later stages of reentry, where flight Mach numbers are comparable to those attainable in wind tunnels, there is fair agreement between flight data and wind-tunnel data. At times where data for the two pressure orifices exist, a comparison of the data indicates a negligible effect of x/l on the afterbody pressure.

In reference 8, wind-tunnel data from several sources were used to correlate p_a/p_∞ with M_∞ for an Apollo-shaped vehicle at $\alpha = 0$. This correlation is reproduced in figure 9; the Fire 1 data have been added and thus the data coverage is extended to $M_\infty = 42$. In the region of $M_\infty = 4$ to $M_\infty = 10$ there are flight data as well as wind-tunnel data, and the two compare favorably as pointed out previously in figure 8. A comparison is also made with calculated curves which were computed by determining the flow direction and isentropic exponent at the body sonic point, and then assuming an isentropic expansion of the flow from the sonic point to the separation line. For these calculations the separation line was assumed to be parallel to the free-stream flow, and the sonic point was obtained from the study of the flow field surrounding the Fire reentry package found in reference 9. Calculations were made for $\gamma_{sp} = 1.2$ and $\gamma_{sp} = 1.4$, which approximates the range of γ_{sp} experienced by the reentry package during reentry. There is fair agreement between the data and the curve for $\gamma_{sp} = 1.4$ in the range of free-stream Mach numbers between 4 and 20 as would be expected. In the vicinity of $M_\infty = 42$ where calculations indicate that γ_{sp} should range between 1.1 and 1.2, the data measured prior to the severe body motions (flagged data) are scattered around the calculated curve for $\gamma_{sp} = 1.2$.

Calorimeter Temperatures

The temperatures measured on the base of the afterbody gold calorimeters are presented in table IV and as a function of time from launch in figure 10. Although the temperatures were measured on the base of the gold calorimeters,

they were treated as average calorimeter temperatures, since the temperature gradients through the highly conductive and thermally thin gold slugs were small. The two thermocouples attached to the base of each gold calorimeter (see fig. 4) measured essentially the same temperature levels during reentry; consequently, temperatures from only one thermocouple are presented in this report. It should also be noted that temperature data were omitted for the calorimeter located at $\phi = 120^\circ$ and $x/l = 0.70$, since telemetry records indicate that these calorimeter thermocouples failed to respond to the heat pulse throughout reentry.

The afterbody temperature as a function of time from launch shown in figure 10 displays some scatter and regions of sparse data, which was attributed to the aforementioned body motions and telemetry signal dropout. In addition, during and after heat-shield ejections the calorimeters were exposed to flow contaminated with ablation products, which affected the data to some degree. As shown in figure 10, the afterbody calorimeter temperatures increased to a maximum at about 1687 seconds and then started a gradual decrease, which indicated that the end of the heat pulse had been reached. The maximum temperature measured on the afterbody was 1350° R and this occurred at $\phi = 120^\circ$ and $x/l = 0.19$. The longitudinal variation of temperature was consistent along all three rays ($\phi = 0^\circ$, 120°, 240°), and the maximum temperatures occurred at $x/l = 0.19$. A decrease in temperature occurred between $x/l = 0.19$ and $x/l = 0.38$ with little variation in temperature thereafter out to $x/l = 0.70$. The circumferential variation in temperatures was less than 75° R in all cases and therefore not considered a dominant effect. The solid curves shown in figure 9 represent an average fairing through the data and were used to calculate the afterbody heating rates which are discussed in the next section.

Afterbody Heating Rates

The afterbody gold calorimeters were designed as simple heat storage experiments, and therefore the heating rates were calculated by using the heat storage equation:

$$\dot{q}_{tot} = \dot{q}_{con} + \alpha_n \dot{q}_{rad} = \frac{m}{S} c_p \frac{dT_a}{dt} + \epsilon_n \sigma T_a^4$$

The assumptions made in using this equation were (1) there was no appreciable temperature gradient through the thin gold slugs; (2) the only significant heat lost was that emitted from the front surface of the calorimeters. These two assumptions were reasonable, since the gold calorimeters had a low thermal diffusion time and were well insulated from the surrounding material. For ease of calculations, a computer program was developed to obtain the total heating rates by using the heat storage equation. The program was set up to fit a polynomial curve to the faired temperature-time curves shown in figure 10 for each calorimeter by using the method of Chebyshev. (See ref. 10.) The analytical derivative was then taken of the resulting polynomial equation, which provided dT_a/dt at any specified time. Additional input into the program necessary to complete the calculations was as follows:

(1) Variation of c_p with temperature - The value of c_p of gold (refs. 13 and 17) was incorporated into the program by using the following equation:

$$c_p = (0.40526 \times 10^{-5})T_a + 0.0284737$$

(2) Mass of each gold slug (m) - This information is presented in table II.

(3) Exposed surface area of each gold slug (S).

(4) Emissivity of oxidized nichrome coating on gold slugs ($\epsilon_n = 0.80$).

(5) Stefan-Boltzmann constant (σ).

The accuracy of the program is entirely dependent on the accuracy of the Chebyshev curve-fit routine and the definition of the material properties of the gold slugs. The curve fits of the Fire 1 temperature-time histories were very accurate and thus provided a reproduction of the faired curves within 2 percent and a comparable scatter in the curve slopes. The material properties of the gold slugs were well defined with the exception of the emissivity of the nichrome surface film. Some experimental work has been done on this surface coating (ref. 12), which made it possible to arrive at a value of 0.80 for the emissivity. The uncertainty in defining the emissivity had little effect on the accuracy of the calculated total heating rates, since the heat reradiated from the calorimeter surface was negligible compared with that stored in the calorimeters throughout reentry. Also, it should be noted that the faired temperature-time curves used in calculating the afterbody heating rates are average curves and tend to smooth the effects of the angle-of-attack variation shown in figure 7.

The afterbody total heating rates calculated by using the heat storage equation are presented in figure 11 as a function of time from launch. The highest heating rates generally occurred in the region of the corner radius. At $x/l = 0.19$ the maximum heating rates ranged between 19 and 25 Btu/ft^2-sec, whereas for the other x/l locations the maximum heating rates were on the order of 14 to 16 Btu/ft^2-sec. There was no indication of a rise in the total heating rates as the apex of the afterbody was approached up to $x/l = 0.70$. Some wind-tunnel data have exhibited this increase in heating rates, which is possibly due to model mounting problems. (See, for example, ref. 6.) The heating rates, like the temperatures, show a small variation with circumferential location.

The times at which the peak heating points occur for each x/l location vary to some degree because of the difficulty in selecting a representative fairing of the temperature-time curves, particularly in the region of inflection.

A summary curve comparing the level of wind-tunnel and theoretical data at 0° angle of attack with the measured flight data is presented in figure 12. In this figure, the ratio of afterbody heating rate to stagnation-point total heating rate is plotted as a function of free-stream Reynolds number for

$x/l = 0.19$. The spread in the ratio of the measured afterbody total heating rates to the measured stagnation total heating rates reflects the accuracy of the measured stagnation total heating rates. (See ref. 2.) In addition, the ratio of the measured afterbody heating rates to the calculated stagnation convective heating rates is shown by the solid curve in the figure. The stagnation convective heating rates were calculated by using the method of reference 13 in conjunction with references 4, 5, and 14 to determine the high-temperature gas properties behind the shock. This curve is included, since it presents the flight data referenced to a parameter which can be readily calculated and is trajectory dependent. Both measured and calculated stagnation heating rates were used as a reference in determining the heating-rate ratios for the wind-tunnel data depending on the source. The wind-tunnel and theoretical data plotted in this figure were obtained from references 6, 8, 9, 15, and 16. It should be noted that this figure is not an attempt at correlating the data, but simply a method for presenting the data from different sources in one figure in order to compare data levels.

An inspection of the flight data in figure 12 indicates that the ratio of afterbody heating rates to stagnation total heating rates $\left(\frac{\left(\dot{q}_{con} + \alpha_n \dot{q}_{rad}\right)_a}{\left(\dot{q}_{con} + \alpha_{be} \dot{q}_{rad}\right)_t}\right)$ reached a maximum in the early stages of flight and decreased as the region of maximum heating was approached. The total-heating-rate ratio reached a minimum in the region of peak reentry heating after which an increasing trend is noted. The variation of afterbody heating rates under normal conditions is controlled by the complex interaction of flow-field parameters such as local enthalpy, Mach number, Reynolds number, and others. In addition to these effects, the Fire 1 afterbody data were affected by angle of attack and contamination of the afterbody flow with ablation products. The presence of angle of attack resulted in an increase in the average heating rate whereas the purging action of the ablation products in the afterbody flow field had a decreasing effect on the heating rates. Due to insufficient data it is very difficult to assess the relative magnitude of these two offsetting effects. In general, however, a comparison of the data presented in this figure shows that the flight data fall generally within the scatter of wind-tunnel and theoretical results.

As shown by the heat storage equation, the afterbody total heating rates are composed of convective and absorbed radiation, which cannot be separated throughout the major portion of reentry. This is due to the fact that after the onset of body motions the task of rigorously interpreting the afterbody radiometer data is virtually impossible because of the lack of roll-rate data. However, prior to the body motions there is a time span for which the total-radiation data are probably accurate and the radiative heating can be separated from the total heating; this separation provides a measure of the afterbody convective heating rates. The sheath of hot gas surrounding the vehicle afterbody was considered optically thin and a gas-geometry correction factor was assumed in determining the total radiation of the surrounding high-temperature air from the essentially normal radiation measured by the onboard instrument. The afterbody gas geometry considered for these calculations was that of a semicylindrical shell of gas radiating to a point at the center of the flat side. The correction factor for this gas configuration is 1.26π (ref. 17).

The radiometer sensed radiation only in the wavelength range above 0.23μ; therefore, it was necessary to assume that there was no contribution to the radiation in the vacuum ultraviolet wavelength range in order to obtain the convective heating component. Flow-field calculations (see ref. 9) support this assumption and thus indicate that the gas temperatures surrounding the afterbody were sufficiently low to preclude the existence of hot air radiation in the vacuum ultraviolet wavelength range. Therefore, for the short time span prior to the onset of body motions, the ratios of radiative and convective heating rates to the combined stagnation radiative and convective heating rates are presented in figure 13 for $\phi = 240^{\circ}$ and $x/l = 0.38$. For the flight conditions indicated, the convective heating rates ranged between 1.5 and 5 percent of the summation of stagnation convective and radiative heating rates. (Note that the reference parameter used is $(\dot{q}_{con} + \dot{q}_{rad})$ rather than $(\dot{q}_{con} + \alpha_{be}\dot{q}_{rad})$.) In comparison, a calculated value of 4 percent was obtained from reference 18 for one discrete point within the range of conditions of the flight data. For these calculations the flow on the afterbody was assumed to be attached. The measured radiative heating component was determined to be very low in comparison and contributed a heating rate of less than 1 percent of the combined stagnation radiative and convective heating rates.

CONCLUDING REMARKS

A reentry flight of an Apollo-shaped vehicle has been performed at a velocity of 37 970 fps and a reentry flight-path angle of -14.5°. The vehicle afterbody was instrumented to obtain total and radiative heating rates as well as limited pressure measurements.

The results indicated that the afterbody pressures measured in flight were in good agreement with available wind-tunnel data up to a Mach number of 10; there was fair agreement with theoretical calculations up to a Mach number of 42.

The ratio of measured afterbody heating rates to measured stagnation total heating rates is generally within the scatter range of wind-tunnel and theoretical results. The maximum heating rate measured on the afterbody during reentry was 23 Btu/ft^2-sec. For a short span of time early in flight, a separation of the radiative and convective heating rates on the afterbody was obtained. During this time the ratio of convective heating rate to the combined stagnation convective and radiative heating rates ranged between 0.015 and 0.05, whereas the radiative heating-rate ratios were less than 0.01.

Langley Research Center,
National Aeronautics and Space Administration,
Langley Station, Hampton, Va., August 12, 1965.

REFERENCES

1. Dingeldein, Richard C.: Flight Measurements of Reentry Heating at Hyperbolic Velocity (Project Fire). NASA TM X-1053, 1965.

2. Cornette, Elden S.: Forebody Temperatures and Total Heating Rates Measured During Project Fire 1 Reentry at 38 000 Feet Per Second. NASA TM X-1120, 1965.

3. Scallion, William I.; and Lewis, John H., Jr.: Flight Parameters and Vehicle Performance for Project Fire Flight 1, Launched April 14, 1964. NASA TN D-2996, 1965.

4. Huber, Paul W.: Hypersonic Shock-Heated Flow Parameters for Velocities to 46,000 Feet Per Second and Altitudes to 323,000 Feet. NASA TR R-163, 1963.

5. Hilsenrath, Joseph; Klein, Max; and Woolley, Harold W.: Tables of Thermodynamic Properties of Air Including Dissociation and Ionization From 1,500° K to 15,000° K. AEDC-TR-59-20, Arnold Eng. Dev. Center, Dec. 1959.

6. Jones, Robert A.: Experimental Investigation of the Overall Pressure Distribution, Flow Field, and Afterbody Heat-Transfer Distribution of an Apollo Reentry Configuration at a Mach Number of 8. NASA TM X-813, 1963.

7. Gray, J. Don; and Jones, J. H.: Force and Pressure Tests on Apollo Configurations at Mach 1.5 Through 10. AEDC-TDR-63-17, U.S. Air Force, Feb. 1963.

8. Lee, George; and Sundell, Robert E.: Heat-Transfer and Pressure Distributions on Apollo Models at $M = 13.8$ in an Arc-Heated Wind Tunnel. NASA TM X-1069, 1965.

9. Brunner, M. J.; Dohner, C. V.; Langelo, V. A.; and Rie, H.: Flow Field Prediction and Analysis - Project Fire. Doc. No. 64SD727 (Contract No. NAS 1-3418), Re-Entry Syst. Dept., Gen. Elec. Co., May 29, 1964.

10. Hamming, R. W.: Numerical Methods for Scientists and Engineers. McGraw-Hill Book Co., Inc., c.1962.

11. Goldsmith, Alexander; Waterman, Thomas E.; and Hirschhorn, Harry J.: Thermophysical Properites of Solid Materials. Volume I - Elements. WADC Tech. Rept. 58-476, Vol. I, U.S. Air Force, Aug. 1960.

12. Gubareff, G. G.; Janssen, J. E.; and Torborg, R. H.: Thermal Radiation Properties Survey. Second ed., Honeywell Res. Center, Minneapolis-Honeywell Regulator Co., 1960.

13. Cohen, Nathaniel B.: Boundary-Layer Similar Solutions and Correlation Equations for Laminar Heat-Transfer Distribution in Equilibrium Air at Velocities up to 41,000 Feet Per Second. NASA TR R-118, 1961.

14. Hansen, C. Frederick: Approximations for the Thermodynamic and Transport Properties of High-Temperature Air. NASA TR R-50, 1959. (Supersedes NACA TN 4150.)

15. Jones, Jim J.; and Moore, John A.: Shock-Tunnel Heat-Transfer Investigation on the Afterbody of an Apollo-Type Configuration at Angles of Attack up to 45°. NASA TM X-1042, 1964.

16. Kuby, W. C.; Byron, S. R.; Foster, R. M.; Hoglund, R. F.; and Hold, M.: Analysis of the Project Fire Re-Entry Package Flow Field. Publ. No. U-3020 (Contract NAS 1-3419), Philco Corp., Oct. 8, 1964.

17. McAdams, William H.: Heat Transmission. Third ed., McGraw-Hill Book Co., Inc., 1954.

18. Stainback, P. Calvin: Convective and Equilibrium Radiation Heat-Transfer Predictions for Project Fire Reentry Vehicle. NASA TN D-2867, 1965.

TABLE I.- AFTERBODY SENSOR LOCATIONS

Station	Afterbody sensors	$\frac{x}{l}$	$(s/R_m)_{av}$
1	Geometric stagnation point	----	0
2	Heat-shield shoulder	0	1.17
3	3 calorimeters (+) ϕ = 0°, 120°, 240°	0.19	1.51
4	1 radiometer (O) ϕ = 203.45°	0.32	1.75
5	3 calorimeters (+) ϕ = 0°, 120°, 240° 1 pressure sensor (Δ) ϕ = 251°	0.38	1.86
6	3 calorimeters (+) ϕ = 0°, 120°, 240°	0.56	2.18
7	3 calorimeters (+) ϕ = 0°, 120°, 240° 1 pressure sensor (Δ) ϕ = 265°	0.70	2.44
8	Theoretical apex of conical afterbody	1.00	2.98

TABLE II.- MASS OF AFTERBODY GOLD CALORIMETERS

Afterbody-calorimeter position		Mass of gold calorimeters, g
ϕ, deg	x/l	
0 ↓	0.19 .38 .56 .70	5.138 5.190 5.168 5.207
120 ↓	0.19 .38 .56	5.235 5.213 4.921
240 ↓	0.19 .38 .56 .70	5.187 5.187 5.235 5.164

TABLE III.- AFTERBODY PRESSURES MEASURED ON FIRE REENTRY PACKAGE

Time from launch, sec	Afterbody pressure, psia	
	$\phi = 251^{\circ}$ $x/l = 0.38$	$\phi = 265^{\circ}$ $x/l = 0.70$
1662.8	-----	0.004
1663.2	-----	.010
1664.4	-----	.031
1665.2	0.026	.042
1665.5	.039	.074
1665.7	-----	.036
1666.0	.011	.018
1666.9	.050	.036
1667.7	.091	.083
1668.1	.071	.089
1687.4	.134	-----
1688.0	.135	.135
1688.2	.124	-----
1688.6	.104	-----
1688.8	.135	.135
1688.9	.130	-----
1689.7	.114	-----
1690.1	.106	-----
1690.5	.109	-----
1690.9	.099	-----
1691.3	.108	-----
1691.7	.109	-----
1692.1	.105	-----
1692.5	.102	-----
1692.9	.102	-----
1693.3	.099	-----
1693.7	.110	-----
1694.1	.094	-----

TABLE IV.- AFTERBODY TEMPERATURES MEASURED ON PROJECT FIRE REENTRY PACKAGE

Time from launch, sec	Afterbody temperatures, ^{o}R										
	$\phi = 0^{o}$				$\phi = 120^{o}$			$\phi = 240^{o}$			
	$\frac{x}{l} = .19$	$\frac{x}{l} = .38$	$\frac{x}{l} = .56$	$\frac{x}{l} = .70$	$\frac{x}{l} = .19$	$\frac{x}{l} = .38$	$\frac{x}{l} = .56$	$\frac{x}{l} = .19$	$\frac{x}{l} = .38$	$\frac{x}{l} = .56$	$\frac{x}{l} = .70$
1650.00	543	550	564	566	543	523	591	552	541	518	561
1650.21	556	556	583	592	567	559	601	558	567	574	580
1650.41	559	559	575	579	559	573	600	552	566	566	579
1650.61	539	539	555	559	541	546	582	548	545	552	557
1650.81	534	552	559	566	539	559	589	536	543	559	557
1651.01	548	539	566	566	550		582	548	543	548	555
1651.21	560	552	573	575	553	557	591	522	557	567	564
1651.42	546	550	575	577	552	557	584	550	527	555	566
1651.62	562	552	580	579	568	573	598	534	555	573	571
1651.82	562	552	580	579	568	573	598	534	555	573	571
1652.02	561	561	579	579	570	570	602	557	561	568	575
1652.22	557	552	579	584	554	568	591	525	559	563	575
1652.42	552	554	568	572	556	563	591	552	554	563	570
1652.63	550	562	575	573	555	566	589	557	559	564	573
1652.83	557	559	575	575	554	570	595	561	565	563	570
1653.03	560	564	585	589	560	564	605	569	564	571	575
1653.23	546	552	563	568	543	559	586	545	545	555	566
1653.43	567	564	585	587	560	571	598	543	560	574	573
1653.63	555	559	579	584	561	561	598	557	561	568	579
1653.83	559	564	582	582	564	561	593	557	561	586	570
1654.05	541	545	557	561	539	550	580	541	539	543	550
1654.26	541	545	557	561	539	550	580	541	539	543	550
1654.46	546	550	561	566	543	555	584	546	543	548	555
1655.26	558	563	574	578	556	567	597	558	556	561	567
1655.47	560	564	576	580	557	569	598	560	557	562	569
1655.85	544	549	560	564	542	553	583	544	542	546	553
1656.05	547	552	563	567	545	556	586	547	545	550	556
1656.25	546	549	560	564	539	550	580	549	540	546	548
1656.68	541	545	557	561	539	550	580	557	549	543	550
1657.27	541	545	559	564	541	553	582	541	539	543	550
1657.48	557	561	572	577	554	566	595	541	539	562	562
1657.72	557	561	572	577	554	566	595	556	554	559	566
1657.96	550	555	566	571	548	559	589	555	551	557	559
1658.19	555	559	571	575	553	564	590	555	553	557	564
1658.39	555	559	571	575	553	564	590	555	553	557	564
1658.62	561	566	577	581	559	570	600	561	559	563	570
1658.82	554	558	569	574	551	563	592	553	551	556	562
1659.03	543	547	558	563	540	552	581	543	540	545	552
1659.40	546	550	561	566	543	555	584	546	543	548	555
1659.60	551	555	566	571	548	559	589	550	548	553	559
1659.80	546	550	561	566	543	555	584	546	543	548	555
1661.01	540	544	555	560	537	549	578	539	537	542	548
1661.21	546	550	561	566	543	555	584	546	543	548	555
1661.41	557	561	572	577	554	566	595	557	554	559	566
1663.02	562	566	565	566	544	550	580	541	539	577	584
1663.23	551	555	566	571	548	559	589	550	548	553	559
1663.43	541	545	557	561	539	550	580	541	539	543	550
1663.61	574	578	589	594	571	583	612	584	564	568	595
1664.42	585	567	591	592	585	595	612	589	581	575	597
1664.62	579	574	583	586	532	580	609	565	576	568	585

TABLE IV. - AFTERBODY TEMPERATURES MEASURED ON PROJECT FIRE REENTRY PACKAGE - Continued

Time from launch, sec	Afterbody temperatures, ^{o}R										
	$\phi = 0^{o}$				$\phi = 120^{o}$			$\phi = 240^{o}$			
	$\frac{x}{l} = .19$	$\frac{x}{l} = .38$	$\frac{x}{l} = .56$	$\frac{x}{l} = .70$	$\frac{x}{l} = .19$	$\frac{x}{l} = .38$	$\frac{x}{l} = .56$	$\frac{x}{l} = .19$	$\frac{x}{l} = .38$	$\frac{x}{l} = .56$	$\frac{x}{l} = .70$
1665.02	612	609	612	632	627	569	614	643	619	624	623
1665.23	613	614	610	627	610	614	654	631	614	603	637
1665.43	633	634	633	648	626	626	662	634	638	624	640
1665.63	628	622	643	567	543	553	659	633	618	604	630
1665.83	647	648	645	665	657	635	683	632	638	627	668
1666.03	647	648	645	665	657	635	683	632	638	627	668
1666.24	647	648	645	665	657	635	683	632	638	627	668
1666.44	643	651	634	654	657	630	663	656	641	611	668
1667.04	653	674	659	690	692	691	732	682	666	661	680
1667.81	692	675	681	704	702	678	738	701	683	663	702
1668.01	710	703	682	708	714	682	719	696	678	664	703
1668.21	711	693	695	730	724	649	723	724	676	728	677
1670.23	781	768	780	787	817	748	810	840	810	752	768
1670.43	790	812	770	784	833	767	815	838	794	746	793
1670.63	820	788	762	778	837	774	844	833	781	749	801
1670.84	846	818	795	807	836	810	813	852	801	758	802
1672.09	887	884	837	915	932	819	879	973	859	750	827
1672.69	903	885	854	884	973	858	887	996	814	861	566
1672.89	925	879	869	880	985	876	901	990	878	810	865
1673.10	925	875	842	881	955	847	872	996	867	798	822
1673.30	939	899	874	896	1013	914	924	998	894	822	873
1673.51	972	925	869	894	1013	874	905	1025	898	841	865
1673.71	987	954	922	937	1041	933	947	1047	900	843	860
1675.31	1063	976	945	983	1103	970	998	1101	949	931	942
1675.52	1061	982	949	956	1085	963	991	1094	976	920	941
1675.72	1060	984	955	977	1093	978	984	1103	966	936	928
1675.92	1054	993	936	967	1089	934	983	1093	963	922	922
1676.12	1060	999	968	997	1122	979	1004	1119	968	952	961
1676.32	1076	986	947	986	1054	964	1003	1113	964	960	957
1676.49	1117	1019	1034	1024	1181	1009	1045	1156	1002	988	992
1676.69	1096	1033	999	995	1157	1019	1019	1147	1012	974	999
1676.89	1053	996	971	999	1099	964	1004	1113	978	958	964
1677.09	1067	996	993	1015	1122	998	1031	1116	971	974	968
1677.30	1127	1019	1029	1055	1179	1027	1049	1179	1025	1012	1006
1677.50	1074	981	966	1014	1143	979	1019	1137	982	964	954
1677.70	1116	1035	1031	1031	1157	1010	1046	1176	1026	1164	1006
1677.90	1094	1033	1040	1070	1168	1037	1074	1186	1033	1019	1054
1678.10	1100	1034	1024	1051	1191	1024		1185	1017	1023	1026
1678.30	1167	1076	1056	1089	1231	1083	1093	1233		1079	1058
1678.50	1136	1054	1050	1083	1194	1046	1080	1179	1035	1058	
1678.71	1142	1053	1030	1082	1199	1123	1064	1193	1038	1034	1067
1678.91	1113	1020	1031	1048	1184	1025	1053	1186	1014	1018	1025
1679.11	1129	1035	1022	1050	1187	991	1068	1202	1029	1033	1027
1679.31	1137	1045	1031	1048	1196	1001	1077	1198	1026	1043	1049
1679.51	1137	1045	1043	1060	1184	1013	1053	1186	1038	1043	1037
1679.71	1137	1069	1068	1072	1220	1061	1113	1198	1062	1055	1073
1679.91	1153	1048	1070	1099	1224	1064	1104	1214	1065	1082	1052
1680.12	1153	1048	1070	1099	1224	1064	1104	1214	1065	1082	1052
1680.32	1170	1066		1105	1228	1058	1110	1230	1059	1064	1070
1680.52	1158	1054	1065	1093	1228	1046	1098	1230	1059	1076	1094

TABLE IV.- AFTERBODY TEMPERATURES MEASURED ON PROJECT FIRE REENTRY PACKAGE - Continued

Time from launch, sec	Afterbody temperatures, ^{o}R										
	$\phi = 0^{o}$				$\phi = 120^{o}$			$\phi = 240^{o}$			
	$\frac{x}{l} = .19$	$\frac{x}{l} = .38$	$\frac{x}{l} = .56$	$\frac{x}{l} = .70$	$\frac{x}{l} = .19$	$\frac{x}{l} = .38$	$\frac{x}{l} = .56$	$\frac{x}{l} = .19$	$\frac{x}{l} = .38$	$\frac{x}{l} = .56$	$\frac{x}{l} = .70$
1680.72	1158	1054	1065	1093	1228	1046	1098	1230	1059	1076	1094
1680.92	1174	1093	1068	1108	1244	1073	1101	1246	1062	1067	1085
1681.12	1174	1081	1080	1120	1208	1073	1101	1246	1026	1103	1097
1681.32	1217	1151	1139	1176	1278	1110	1160	1258		1116	1155
1681.53	1182	1018	1089	1117	1240	1082	1123	1254	1059	1076	1082
1681.73	1162	1093	1104	1108	1232	1061	1101	1258	1074	1115	1097
1681.93	1162	1093	1104	1108	1232	1061	1101	1258	1074	1115	1097
1682.13	1089	1093	1104	1132	1268	1098	1150	1258	1074	1115	1097
1682.33	1218	1071	1129	1151	1243	1111	1150	1244	1084	1177	1126
1682.53	1197	1106	1113	1165	1302	1129	1183	1268	1091	1126	1126
1682.73	1234	1141	1137	1162	1274	1165	1183	1260	1132	1175	1169
1682.94	1234	1141	1137	1162	1274	1165	1183	1260	1132	1175	1169
1683.14	1243	1124	1188	1166	1293	1109	1249	1251	1141	1156	1164
1683.34	1265	1136	1159	1176	1300	1147	1183	1249	1095	1111	1144
1683.54	1237	1135	1164	1189	1271	1130	1174	1279	1123	1160	1142
1683.74	1240	1122	1121	1192	1275	1105	1203	1239	1106	1048	1127
1683.94	1197	1115	1126	1167	1281	1082	1172	1197	1071	1150	1156
1684.14	1256	1147	1145	1190	1296	1147	1188	1266	1125	1183	1168
1684.35	1297	1177	1152		1316	1156	1203	1288	1134	1208	1201
1684.55	1308	1178	1201	1222	1342	1187	1219	1295	1143	1203	1228
1684.75	1262	1149	1145	1181	1268	1141	1198	1270	1105	1172	1185
1684.95	1245	1121	1127	1172	1305	1132	1228		1110	1157	1168
1685.15	1281	1184	1180	1230	1302	1172	1208	1275	1134	1184	1234
1685.35	1308	1156	1148	1184	1294	1167	1155	1271	1141	1167	1173
1685.55	1234	1093	1128	1157	1268	1098	1126	1246	1050	1164	1170
1685.76	1226	1108	1131	1172	1248	1088	1153	1250	1102	1155	1161
1685.96	1238	1147	1136	1185	1256	1104	1176	1258	1116	1168	1197
1686.16	1218	1157	1176	1212	1278	1130	1200	1249	1092	1161	1178
1686.36	1287	1136	1168	1203	1273	1136	1154	1281	1132	1184	1165
1686.56	1225	1115	1136	1207	1253	1107	1161	1249	1098	1149	1129
1686.76	1254	1155	1168	1207	1264	1153	1177	1254	1111	1176	1162
1686.96	1273	1156	1157	1178	1252	1161	1159	1265	1118	1188	1202
1687.50	1325	1199	1223	1263	1351	1204	1247	1316	1168	1228	1250
1687.70	1264	1141	1160	1208	1295	1151	1188	1264	1107	1176	1189
1687.90	1286	1158	1171	1214	1297	1162	1203	1273	1119	1193	1206
1688.10	1263	1146	1168	1203	1280	1157	1183	1261	1116	1166	1198
1688.30	1269	1134	1161	1214	1304	1161	1205	1282	1128	1197	1208
1688.51	1281	1166	1181	1213	1307	1164	1211	1270	1126	1201	1205
1688.71	1296	1176	1196	1230	1318	1174	1216	1298	1145	1210	1219
1688.91	1278	1155	1181	1201	1287	1139	1185	1276	1126	1199	1208
1689.11	1280	1157	1181	1216	1304	1159	1198	1269	1130	1199	1207
1689.31	1292	1162	1197	1231	1307	1164	1215	1276	1138	1212	1213
1689.51	1243	1123	1146	1184	1265	1127	1176	1236	1091	1158	1169
1689.72	1262	1135	1163	1198	1286	1148	1183	1251	1107	1177	1194
1689.92	1263	1143	1174	1214	1300	1164	1207	1257	1109	1178	1191
1690.12	1238	1127	1144	1182	1265	1130	1170	1240	1088	1159	1176
1690.32	1255	1137	1157	1196	1278	1142	1181	1248	1105	1170	1183
1690.52	1254	1140	1167	1198	1278	1144	1181	1251	1113	1177	1194
1690.72	1247	1127	1151	1183	1268	1134	1168	1236	1099	1164	1173
1690.92	1243	1121	1147	1178	1269	1132	1171	1239	1095	1160	1173

TABLE IV.- AFTERBODY TEMPERATURES MEASURED ON PROJECT FIRE REENTRY PACKAGE - Continued

Time from launch, sec	Afterbody temperatures, ^{o}R										
	$\phi = 0^{o}$				$\phi = 120^{o}$			$\phi = 240^{o}$			
	$\frac{x}{l} = .19$	$\frac{x}{l} = .38$	$\frac{x}{l} = .56$	$\frac{x}{l} = .70$	$\frac{x}{l} = .19$	$\frac{x}{l} = .38$	$\frac{x}{l} = .56$	$\frac{x}{l} = .19$	$\frac{x}{l} = .38$	$\frac{x}{l} = .56$	$\frac{x}{l} = .70$
1691.13	1231	1122	1152	1173	1258	1131	1168	1228	1097	1161	1173
1691.33	1242	1129	1152	1191	1271	1129	1161	1237	1108	1161	1180
1691.53	1228	1115	1136	1177	1258	1121	1154	1224	1087	1153	1164
1691.73	1256	1144	1163	1190	1281	1142	1178	1247	1112	1182	1190
1691.93	1239	1130	1151	1181	1269	1136	1169	1226	1100	1170	1181
1692.13	1221	1114	1141	1176	1271	1137	1170	1220	1079	1152	1163
1692.34	1202	1089	1113	1151	1242	1111	1147	1204	1070	1142	1145
1692.54	1207	1100	1125	1159	1243	1106	1138	1205	1076	1140	1152
1692.74	1197	1093	1123	1159	1244	1106	1141	1204	1059	1134	1144
1692.94	1210	1105	1111	1145	1229	1096	1127	1202	1077	1143	1151
1693.14	1217	1106	1132	1166	1246	1115	1147	1210	1085	1149	1151
1693.34	1203	1091	1119	1138	1228	1091	1128	1203	1059	1129	1136
1693.55	1191	1086	1118	1139	1225	1099	1135	1200	1073	1139	1134
1693.75	1206	1099	1125	1159	1242	1112	1144	1201	1076	1138	1146
1693.95	1197	1100	1125	1159	1233	1108	1141	1197	1061	1138	1142
1694.15	1193	1092	1117	1149	1237	1109	1133	1199	1066	1138	1145
1694.35	1204	1086	1105	1147	1231	1107	1137	1193	1073	1134	1143
1694.55	1187	1076	1107	1133	1222	1093	1121	1185	1055	1120	1132
1694.75	1200	1095	1123	1155	1231	1115	1138	1193	1070	1140	1151
1694.96	1197	1089	1121	1153	1233	1108	1136	1191	1072	1131	1142
1695.16	1185	1087	1115	1141	1225	1102	1128	1181	1055	1130	1130
1695.36	1186	1085	1108	1130	1222	1096	1128	1187	1061	1130	1134
1695.56	1180	1083	1110	1136	1221	1091	1128	1180	1057	1119	1123
1695.76	1187	1082	1114	1133	1227	1107	1133	1177	1057	1116	1126
1695.96	1181	1066	1098	1121	1204	1092	1109	1170	1045	1104	1111
1696.17	1183	1080	1110	1131	1234	1099	1119	1189	1056	1110	1138
1696.37	1177	1061	1091	1129	1202	1084	1117	1160	1038	1103	1105
1696.57	1168	1083	1106	1129	1226	1093	1117	1179	1059	1118	1137
1696.77	1181	1061	1109	1135	1218	1094	1113	1162	1055	1120	1118
1696.97	1149	1063	1091	1120	1197	1080	1110	1157	1029	1093	1101
1697.17	1184	1086	1128	1149	1227	1107	1137	1184	1073	1134	1138
1697.38	1162	1062	1096	1117	1202	1081	1109	1162	1030	1098	1115
1697.58	1159	1062	1096	1115	1197	1083	1107	1159	1045	1100	1111
1697.78	1179	1093	1118	1141	1227	1107	1133	1183	1063	1124	1135
1697.98	1149	1049	1076	1110	1193	1082	1102	1151	1034	1095	1099
1698.18	1150	1050	1082	1112	1197	1076	1102	1142	1033	1097	1106
1698.38	1143	1047	1081	1102	1189	1072	1098	1150	1036	1097	1097
1698.58	1145	1053	1088	1109	1198	1077	1099	1143	1030	1087	1104
1698.79	1161	1069	1096	1121	1198	1090	1116	1155	1046	1102	1117
1698.99	1142	1038	1074	1093	1180	1066	1088	1129	1030	1081	1085
1699.19	1148	1044	1082	1097	1186	1072	1093	1146	1029	1084	1097
1699.39	1138	1033	1073	1094	1180	1064	1084	1132	1022	1081	1090
1699.59	1139	1041	1077	1097	1179	1069	1091	1130	1016	1079	1080
1699.79	1137	1044	1082	1099	1183	1072	1087	1139	1027	1086	1093
1700.00	1155	1064	1098	1114	1201	1085	1111	1145	1047	1103	1112
1700.20	1135	1038	1072	1091	1179	1067	1087	1133	1019	1078	1089
1700.40	1140	1037	1067	1090	1176	1069	1084	1131	1017	1079	1082
1700.60	1122	1029	1061	1080	1165	1059	1076	1119	1006	1071	1082
1700.80	1132	1038	1059	1089	1172	1063	1083	1119	1009	1076	1086
1701.00	1127	1040	1074	1091	1171	1061	1083	1122	1010	1076	1091

TABLE IV.- AFTERBODY TEMPERATURES MEASURED ON PROJECT FIRE REENTRY PACKAGE - Continued

Time from launch, sec	Afterbody temperatures, ^{o}R										
	$\phi = 0^{o}$				$\phi = 120^{o}$			$\phi = 240^{o}$			
	$\frac{x}{l} = .19$	$\frac{x}{l} = .38$	$\frac{x}{l} = .56$	$\frac{x}{l} = .70$	$\frac{x}{l} = .19$	$\frac{x}{l} = .38$	$\frac{x}{l} = .56$	$\frac{x}{l} = .19$	$\frac{x}{l} = .38$	$\frac{x}{l} = .56$	$\frac{x}{l} = .70$
1701.20	1114	1028	1059	1082	1159	1055	1079	1113	1015	1072	1074
1701.41	1133	1040	1068	1087	1174	1066	1088	1126	1020	1077	1079
1701.61	1114	1025	1059	1069	1161	1052	1063	1112	1005	1054	1072
1701.81	1105	1018	1046	1069	1156	1044	1063	1103	997	1054	1063
1702.01	1117	1027	1059	1081	1166	1057	1075	1117	1014	1066	1074
1702.21	1115	1025	1059	1078	1157	1046	1070	1115	1010	1058	1073
1702.41	1135	1052	1083	1100	1183	1079	1097	1139	1025	1087	1092
1702.61	1134	1050	1078	1099	1178	1073	1089	1130	1025	1082	1084
1702.82	1100	1011	1045	1056	1144	1035	1057	1096	988	1047	1054
1703.02	1108	1017	1051	1068	1150	1045	1060	1097	1006	1055	1066
1703.22	1104	1009	1043	1062	1147	1039	1058	1098	994	1047	1056
1703.42	1098	1012	1049	1066	1150	1040	1058	1107	993	1053	1062
1703.62	1111	1024	1061	1076	1156	1052	1068	1106	1003	1061	1065
1703.82	1086	1006	1046	1053	1134	1036	1055	1088	991	1044	1050
1704.02	1078	999	1035	1049	1129	1028	1052	1080	980	1032	1039
1704.23	1087	1016	1045	1058	1141	1043	1059	1099	980	1039	1052
1704.43	1093	1005	1031	1050	1135	1031	1053	1091	988	1042	1052
1704.63	1100	1011	1044	1063	1147	1040	1057	1096	992	1050	1057
1704.83	1086	1004	1038	1055	1135	1029	1051	1088	991	1044	1046
1705.03	1086	1001	1035	1046	1132	1023	1051	1077	978	1033	1037
1705.23	1082	1001	1039	1048	1130	1029	1048	1081	990	1039	1043
1705.44	1087	996	1026	1047	1123	1028	1043	1072	979	1032	1040
1705.64	1076	996	1024	1045	1121	1026	1043	1087	977	1028	1036
1705.84	1065	994	1013	1035	1123	1020	1030	1080	972	1026	1037
1706.04	1076	987	1027	1040	1122	1023	1036	1069	980	1031	1038
1706.24	1066	987	1020	1039	1110	1014	1034	1075	972	1026	1029
1706.44	1069	994	1022	1039	1118	1018	1037	1062	973	1024	1031
1706.64	1089	1012	1042	1058	1132	1043	1059	1095	991	1043	1048
1706.85	1102	1019	1051	1064	1146	1049	1066	1106	1000	1057	1059
1707.05	1100	1022	1060	1066	1150	1045	1065	1100	1003	1056	1062
1707.25	1092	1011	1043	1056	1138	1041	1054	1087	996	1049	1054
1707.45	1081	1005	1034	1048	1128	1030	1049	1083	988	1038	1044
1707.65	1057	984	1015	1022	1110	1011	1031	1055	952	1003	1020
1707.85	1063	988	1020	1026	1106	1009	1029	1073	970	1013	1024
1708.06	1061	974	1013	1019	1106	1002	1028	1046	964	1006	1019
1708.26	1081	1009	1036	1053	1135	1038	1054	1087	991	1034	1043
1708.46	1070	995	1029	1035	1119	1020	1042	1069	978	1030	1037
1708.66	1040	972	1011	1025	1089	1004	1024	1046	961	1000	1006
1708.86	1071	995	1031	1033	1110	1020	1040	1067	983	1022	1030
1709.06	1053	975	1003	1023	1100	1003	1025	1059	960	993	1005
1709.26	1053	973	1002	1019	1097	1000	1018	1053	953	1002	1013
1709.47	1062	982	1018	1029	1114	1016	1036	1064	974	1020	1031
1709.67	1037	962	994	1009	1087	990	1010	1039	947	999	1003
1709.87	1041	965	1005	1014	1090	992	1012	1047	950	997	1007
1710.07	1037	965	999	1003	1084	991	1006	1044	950	995	1008
1710.27	1034	962	991	1000	1082	989	1011	1038	944	987	998
1710.47	1033	961	993	1003	1083	988	1008	1037	944	990	999
1710.68	1036	960	992	1002	1083	988	1001	1029	945	992	1002
1710.88	1014	951	983	993	1070	980	992	1020	936	974	993
1711.08	1033	953	989	1002	1077	989	1004	1026	938	989	993

TABLE IV.- AFTERBODY TEMPERATURES MEASURED ON PROJECT FIRE REENTRY PACKAGE - Continued

Time from launch, sec	Afterbody temperatures, ^{o}R										
	$\phi = 0^{o}$				$\phi = 120^{o}$			$\phi = 240^{o}$			
	$\frac{x}{l} = .19$	$\frac{x}{l} = .38$	$\frac{x}{l} = .56$	$\frac{x}{l} = .70$	$\frac{x}{l} = .19$	$\frac{x}{l} = .38$	$\frac{x}{l} = .56$	$\frac{x}{l} = .19$	$\frac{x}{l} = .38$	$\frac{x}{l} = .56$	$\frac{x}{l} = .70$
1711.28	1054	985	1015	1023	1100	1008	1028	1054	968	1004	1021
1711.48	1029	955	987	996	1075	983	1003	1031	941	987	991
1711.68	1031	958	988	997	1078	989	1004	1027	939	984	995
1711.88	1026	950	982	992	1075	980	999	1020	939	979	988
1712.09	1018	946	978	982	1062	965	985	1016	925	976	971
1712.29	1041	974	1003	1013	1093	999	1020	1037	938	994	1009
1712.49	1011	941	973	982	1055	967	989	1009	922	973	973
1712.69	1014	946	976	988	1062	974	993	1020	931	969	980
1712.89	1016	947	980	988	1067	969	988	1018	934	977	984
1713.09	1037	971	1004	1013	1089	1000	1009	1043	952	994	1002
1713.30	1017	947	983	999	1074	978	998	1017	935	980	987
1713.50	1009	942	974	984	1061	965	991	1017	933	974	984
1713.70	1024	964	993	1004	1078	985	1009	1032	947	991	993
1713.90	1007	938	970	978	1056	963	976	1016	925	963	972
1714.10	1006	940	962	977	1055	966	979	1017	919	968	974
1714.30	1004	932	962	972	1052	960	977	993	919	962	970
1714.50	994	930	960	968	1051	953	975	995	896	936	949
1714.71	983	920	950	960	1036	945	965	996	901	952	960
1714.91	996	934	963	976	1048	957	981	996	925	956	967
1715.11	1007	941	971	980	1055	969	984	1015	922	960	967
1715.31	998	922	958	968	1044	954	973	995	913	947	966
1715.51	996	923	958	973	1045	956	971	994	911	956	960
1715.71	985	915	947	962	1038	945	962	987	890	945	951
1715.92	986	927	961	965	1045	952	970	990	908	952	963
1716.12	1004	944	969	980	1058	973	989	1010	925	963	973
1716.32	1021	958	983	994	1067	981	997	1027	941	981	985
1716.52	982	921	948	961	1033	942	964	990	899	944	950
1716.72	986	914	942	959	1029	944	966	975	900	944	946
1716.92	979	912	946	956	1028	937	957	990	903	939	948
1717.13	979	921	947	951	1025	942	960	989	906	940	947
1717.33	987	924	945	949	1027	951	967	993	904	953	949
1717.53	981	917	945	958	1030	941	963	983	898	941	949
1717.73	960	900	932	932	1012	921	954	970	891	930	928
1717.93	968	911	937	954	1018	935	940	974	894	930	943
1718.13	968	911	947	951	1016	947	962	976	904	945	947
1718.33	967	910	936	946	1022	938	955	976	897	933	940
1718.54	976	908	938	950	1022	938	955	973	893	935	935
1718.74	993	934	962	975	1046	964	979	1006	919	958	966
1718.94	966	908	930	942	1020	934	951	970	872	917	936
1719.14	970	909	943	951	1018	932	956	968	896	938	938
1719.34	995	938	965	976	1053	965	981	1004	925	963	961
1719.54	955	904	927	933	1006	923	936	963	888	921	929
1719.75	993	933	958	966	1043	954	973	993	913	953	960
1719.95	968	902	935	945	1017	935	952	966	890	924	941
1720.15	959	899	934	942	1017	934	951	974	886	925	934
1720.35	981	922	954	966	1031	943	967	981	911	953	945
1720.55	962	904	938	938	1009	927	955	974	888	927	936
1720.75	954	902	926	934	1009	928	945	960	878	921	924
1720.95	969	906	936	947	1014	932	951	967	895	926	936
1721.16	962	897	932	938	1011	923	947	970	882	923	934

TABLE IV. - AFTERBODY TEMPERATURES MEASURED ON PROJECT FIRE REENTRY PACKAGE - Continued

Time from launch, sec	Afterbody temperatures, ^{o}R										
	$\phi = 0^{o}$				$\phi = 120^{o}$			$\phi = 240^{o}$			
	$\frac{x}{l} = .19$	$\frac{x}{l} = .38$	$\frac{x}{l} = .56$	$\frac{x}{l} = .70$	$\frac{x}{l} = .19$	$\frac{x}{l} = .38$	$\frac{x}{l} = .56$	$\frac{x}{l} = .19$	$\frac{x}{l} = .38$	$\frac{x}{l} = .56$	$\frac{x}{l} = .70$
1721.36	961	901	929	944	1003	931	949	948	882	927	929
1721.56	958	902	928	940	1012	921	951	951	884	921	930
1721.76	971	912	934	942	1014	934	958	960	897	934	938
1721.96	971	914	944	955	1016	940	962	982	902	938	944
1722.16	955	900	920	926	1000	920	935	957	876	913	922
1722.37	940	886	912	922	988	903	925	944	867	905	912
1722.57	931	881	914	924	982	899	925	943	862	909	903
1722.77	950	894	926	932	999	918	941	956	879	917	926
1722.97	949	896	918	929	999	918	937	957	877	912	920
1723.17	940	882	912	921	984	914	930	948	865	901	906
1723.37	936	883	909	927	993	912	929	949	866	910	914
1723.58	939	890	917	926	993	907	931	943	870	913	915
1723.78	944	884	916	920	989	905	933	935	873	908	914
1723.98	960	906	933	940	997	925	953	960	891	929	935
1724.18	937	881	905	922	984	905	928	928	868	898	905
1724.38	968	916	937	950	1012	935	955	965	894	931	942
1724.58	926	876	900	915	979	900	915	932	861	894	902
1724.79	952	894	925	934	997	925	945	956	885	927	925
1724.99	920	878	899	910	969	897	921	933	862	895	895
1725.19	920	867	897	905	970	893	918	918	849	890	892
1725.39	948	895	923	932	990	921	939	963	881	912	925
1725.59	914	859	891	900	960	889	909	916	850	879	889
1725.79	911	864	894	900	962	892	914	928	852	888	892
1725.99	924	875	905	913	966	901	922	926	859	896	903
1726.20	922	869	895	901	963	893	916	905	847	884	895
1726.40	917	873	895	903	968	891	912	908	853	893	893
1726.60	949	900	927	938	996	925	945	955	880	915	923
1726.80	928	878	900	917	978	904	921	935	865	900	902
1727.00	918	868	896	911	963	896	915	922	854	885	892
1727.20	933	893	923	925	984	912	932	926	874	908	908
1727.41	940	893	923	932	987	919	934	931	876	910	917
1727.61	899	843	878	887	946	880	898	914	836	872	876
1727.81	912	841	889	900	954	883	907	899	852	885	891
1728.01	910	867	895	899	960	891	908	923	851	884	893
1728.21	931	884	912	925	975	914	936	937	869	908	912
1728.41	900	856	878	889	941	879	902	913	840	872	876
1728.61	908	864	890	896	955	888	903	920	846	879	881
1728.82	906	858	886	897	954	882	904	915	846	880	891
1729.02	892	849	880	890	945	873	897	907	838	871	878
1729.22	905	859	886	896	951	881	905	899	834	875	884
1729.42	907	862	878	891	948	887	906	906	842	880	880
1729.62	891	838	870	876	935	869	891	895	825	863	867
1729.82	887	840	866	879	927	864	884	895	826	860	864
1730.03	902	866	887	893	946	881	907	904	845	881	885
1730.23	891	847	874	880	938	874	895	903	838	865	867
1730.43	886	838	863	871	925	863	885	886	818	856	865
1730.63	906	866	888	898	945	888	911	900	846	881	883
1730.83	912	870	895	906	949	895	909	914	856	887	893
1731.03	875	833	862	871	919	857	882	881	821	851	855
1731.24	898	850	881	885	933	879	892	906	836	868	870

TABLE IV.- AFTERBODY TEMPERATURES MEASURED ON PROJECT FIRE REENTRY PACKAGE - Continued

Time from launch, sec	Afterbody temperatures, ^{o}R										
	$\phi = 0^{o}$				$\phi = 120^{o}$			$\phi = 240^{o}$			
	$\frac{x}{l} = .19$	$\frac{x}{l} = .38$	$\frac{x}{l} = .56$	$\frac{x}{l} = .70$	$\frac{x}{l} = .19$	$\frac{x}{l} = .38$	$\frac{x}{l} = .56$	$\frac{x}{l} = .19$	$\frac{x}{l} = .38$	$\frac{x}{l} = .56$	$\frac{x}{l} = .70$
1731.44	888	841	868	877	929	868	892	892	832	859	861
1731.64	900	856	884	890	941	884	901	908	842	875	883
1731.84	877	835	857	868	924	859	875	877	819	844	861
1732.04	905	861	887	897	936	882	904	907	852	882	888
1732.24	874	832	856	863	913	858	879	880	821	841	852
1732.44	897	857	883	894	940	889	882	889	846	879	881
1732.65	863	826	850	857	908	850	866	874	819	846	852
1732.85	865	825	850	858	901	847	868	876	811	838	849
1733.05	868	830	859	868	913	850	879	881	816	848	850
1733.25	870	825	854	865	906	856	876	874	816	847	845
1733.45	871	831	853	864	909	857	880	877	815	844	848
1733.65	860	822	840	845	902	842	865	869	809	833	838
1733.86	854	817	841	854	901	841	868	854	805	837	839
1734.06	865	827	852	863	910	850	877	885	818	845	856
1734.26	862	817	847	860	884	829	851	875	813	842	840
1734.46	842	815	844	846	897	844	873	870	806	839	837
1734.66	873	845	860	875	916	867	889	889	823	855	860
1734.86	841	816	834	841	898	841	866	859	796	837	832
1735.07	848	812	832	839	891	837	859	850	796	830	836
1735.27	867	839	878	890	922	861	896	887	828	865	865
1735.47	834	798	823	827	879	825	850	862	765	814	825
1735.67	851	819	844	848	902	842	873	851	810	835	840
1735.87	840	808	826	840	888	833	853	860	790	822	831
1736.07	867	839	859	870	916	857	883	884	828	859	863
1736.28	860	830	854	867	905	854	879	877	826	852	852
1736.48	843	814	841	836	890	836	864	849	803	827	839
1736.68	842	815	833	840	885	837	862	859	804	828	833
1736.88	833	811	829	840	890	829	858	851	788	820	829
1737.08	832	805	828	832	875	825	844	847	788	819	823
1737.28	825	799	823	830	875	821	855	836	788	803	819
1737.48	866	837	857	866	902	855	878	875	824	851	853
1737.69	821	799	824	830	879	824	851	830	788	810	821
1737.89	832	807	821	834	871	823	846	847	787	814	818
1738.09	821	792	821	823	869	819	844	834	783	808	817
1738.29	825	794	812	823	862	819	846	823	788	812	812
1738.49	831	793	820	825	878	816	852	849	784	811	813
1738.69	817	792	808	821	860	812	833	835	785	805	819
1738.90	824	790	819	826	874	817	851	828	788	817	821
1739.10	853	827	847	851	891	845	870	844	814	836	847
1739.30	861	838	850	861	901	852	879	873	818	847	849
1739.50	872	836	852	861	908	861	877	870	814	832	852
1739.70	831	797	812	824	871	817	835	837	776	803	810
1739.90	828	799	815	830	865	826	844	837	783	808	817
1740.10	827	800	811	829	866	822	841	842	785	805	814
1740.31	850	813	829	838	879	840	854	852	798	820	827
1740.51	842	820	834	847	881	843	861	849	803	827	829
1740.71	807	778	800	804	846	800	827	822	773	787	798
1740.91	818	793	813	820	860	809	834	831	779	795	802
1741.11	816	789	805	814	856	814	821	823	780	792	801
1741.31	811	780	802	809	850	809	829	822	771	791	800

TABLE IV.- AFTERBODY TEMPERATURES MEASURED ON PROJECT FIRE REENTRY PACKAGE - Continued

Time from launch, sec	Afterbody temperatures, ^{o}R										
	$\phi = 0^{o}$				$\phi = 120^{o}$			$\phi = 240^{o}$			
	$\frac{x}{l} = .19$	$\frac{x}{l} = .38$	$\frac{x}{l} = .56$	$\frac{x}{l} = .70$	$\frac{x}{l} = .19$	$\frac{x}{l} = .38$	$\frac{x}{l} = .56$	$\frac{x}{l} = .19$	$\frac{x}{l} = .38$	$\frac{x}{l} = .56$	$\frac{x}{l} = .70$
1741.52	812	790	806	815	852	804	829	828	777	797	799
1741.72	812	786	797	806	852	808	828	817	776	790	797
1741.92	811	782	794	805	842	805	819	813	756	778	785
1742.12	809	779	800	808	851	806	816	815	770	788	793
1742.32	810	783	803	803	843	798	821	818	765	787	794
1742.52	833	813	827	835	871	831	852	841	793	811	820
1742.73	809	780	800	811	849	805	823	807	758	760	789
1742.93	804	777	790	806	839	795	811	801	761	779	790
1743.13	804	779	795	806	847	800	816	815	766	786	788
1743.33	801	775	790	795	834	795	813	808	759	775	784
1743.53	805	774	796	801	836	799	817	814	763	776	787
1743.73	801	770	781	795	834	792	813	796	748	772	779
1743.93	803	771	794	800	836	800	814	809	753	780	789
1744.14	808	783	797	803	842	801	822	819	770	788	792
1744.34	787	767	781	785	820	783	806	798	749	772	772
1744.54	835	800	815	829	865	822	842	835	786	804	815
1744.74	817	795	807	820	856	815	829	826	773	795	802
1744.94	797	775	786	797	828	786	811	797	750	779	781
1745.14	784	762	775	780	824	784	800	795	748	735	764
1745.35	792	770	777	790	831	792	808	794	750	774	770
1745.55	807	779	793	803	842	803	820	814	768	786	790
1745.75	782	753	771	786	820	784	796	791	750	766	766
1745.95	796	792	790	803	842	803	819	807	765	783	785
1746.15	808	789	791	807	841	804	818	791	769	787	791
1746.35	784	757	769	777	817	777	802	788	748	757	766
1746.56	801	782	797	810	840	799	820	805	773	790	793
1746.76	802	787	799	803	839	798	828	809	778	783	790
1746.96	774	741	754	770	804	763	786	780	736	748	756
1747.16	810	786	797	804	843	804	822	817	768	788	793
1747.36	776	756	754	771	811	769	790	780	733	754	758
1747.56	778	755	767	778	806	775	787	786	740	753	760
1747.76	770	752	761	770	803	772	788	765	736	754	756
1747.97	752	743	733	746	785	748	780	772	732	743	752
1748.17	787	758	767	783	818	781	799	765	743	754	763
1748.37	766	744	756	769	801	762	785	777	740	749	751
1748.57	762	746	746	762	795	758	778	755	731	740	742
1748.77	767	751	756	776	802	778	792	751	715	742	744
1748.97	760	733	739	755	793	755	776	769	737	748	751
1749.18	760	740	751	760	795	758	776	767	729	745	751
1749.38	769	749	755	767	806	767	789	766	737	742	746
1749.58	760	737	751	758	788	753	778	766	728	738	738
1749.78	766	748	750	757	803	766	782	770	721	739	741
1749.98	760	740	745	762	794	758	774	765	726	738	742
1750.18	758	740	745	765	798	758	776	765	729	740	745
1750.38	764	749	751	764	806	771	785	762	729	740	733
1750.59	751	737	736	749	790	755	763	762	717	729	735
1750.79	762	742	744	755	793	755	769	764	724	737	746
1750.99	760	745	747	765	798	758	774	753	722	738	729
1751.19	772	750	746	763	803	770	782	752	739	746	750
1751.39	752	734	734	745	783	757	764	757	716	721	736

TABLE IV. - AFTERBODY TEMPERATURES MEASURED ON PROJECT FIRE REENTRY PACKAGE - Continued

Time from launch, sec	Afterbody temperatures, °R										
	$\phi = 0^\circ$				$\phi = 120^\circ$			$\phi = 240^\circ$			
	$\frac{x}{l} = .19$	$\frac{x}{l} = .38$	$\frac{x}{l} = .56$	$\frac{x}{l} = .70$	$\frac{x}{l} = .19$	$\frac{x}{l} = .38$	$\frac{x}{l} = .56$	$\frac{x}{l} = .19$	$\frac{x}{l} = .38$	$\frac{x}{l} = .56$	$\frac{x}{l} = .70$
1751.59	780	749	760	771	804	776	792	780	749	758	758
1751.80	775	766	768	764	810	781	795	781	754	750	766
1752.00	761	739	744	757	794	759	773	754	717	724	737
1752.20	759	741	744	757	794	753	773	759	723	735	739
1752.40	748	734	741	750	779	757	771	743	723	719	737
1752.60	732	732	734	728	769	730	753	754	719	721	728
1752.80	740	717	722	742	770	733	751	746	711	715	718
1753.00	745	727	725	743	774	741	757	747	704	723	727
1753.21	739	719	719	737	770	735	737	728	710	714	714
1753.41	788	762	763	782	813	794	798	755	717	760	760
1753.61	755	738	727	740	772	742	761	716	703	727	725
1753.81	725	722	724	717	767	733	745	724	699	709	718
1754.01	750	736	736	750	780	754	768	749	718	727	730
1754.21	732	711	718	721	753	725	737	738	709	707	714
1754.42	733	720	717	733	764	731	754	735	706	708	720
1754.62	734	718	725	734	767	743	754	736	709	712	714
1754.82	732	721	717	725	761	734	750	705	703	705	712
1755.02	765	756	748	763	795	765	782	763	732	737	743
1755.22	742	724	733	740	769	738	756	733	709	711	713
1755.42	762	745	749	756	783	760	777	766	734	738	749
1755.63	753	735	733	747	781	753	767	774	737	744	748
1755.83	727	709	711	727	756	725	738	722	698	707	711
1756.03	731	714	718	729	757	729	750	729	696	707	712
1756.23	720	708	700	718	744	717	740	724	693	697	702
1756.43	734	728	728	734	765	741	753	707	699	712	717
1756.63	722	711	709	722	750	726	734	735	695	700	709
1756.83	728	718	716	723	757	732	746	700	696	703	709
1757.04	742	726	731	737	771	738	758	735	710	715	720
1757.24	750	735	729	740	759	733	745	739	728	724	733
1757.44	726	706	706	721	752	721	735	725	699	701	706
1757.64	718	707	703	716	742	722	730	715	695	698	707
1757.84	717	701	698	714	749	719	730	719	689	692	696
1758.04	751	735	727	745	775	747	765	749	720	727	725
1758.25	714	701	690	703	732	705	726	712	692	694	701
1758.45	717	712	699	717	743	719	740	725	701	695	693
1758.65	725	712	712	716	745	730	741	729	694	699	708
1758.85	717	701	703	708	737	715	708	721	696	683	697
1759.05	694	698	703	709	736	718	710	696	676	669	674
1759.25	738	720	724	733	758	742	749	718	709	704	718
1759.46	742	725	725	736	763	740	759	748	716	714	725
1759.66	705	693	696	692	722	687	719	711	682	682	698
1759.86	702	695	700	706	728	713	729	691	686	682	675
1760.06	748	730	731	733	763	742	758	750	724	717	720
1760.26	709	691	684	700	726	704	720	675	679	677	689
1760.46	710	694	692	701	729	708	726	710	687	685	690
1760.67	722	713	711	711	747	731	740	704	702	695	702
1760.87	697	677	688	686	717	699	706	708	683	675	681
1761.07	711	716	716	727	754	732	748	711	691	698	702
1761.27	700	684	685	689	719	700	707	700	673	667	676
1761.47	705	667	660	671	707	685	698	702	675	673	678

TABLE IV. - AFTERBODY TEMPERATURES MEASURED ON PROJECT FIRE REENTRY PACKAGE - Continued

Time from launch, sec	Afterbody temperatures, ^{o}R										
	$\phi = 0^{o}$				$\phi = 120^{o}$			$\phi = 240^{o}$			
	$\frac{x}{l} = .19$	$\frac{x}{l} = .38$	$\frac{x}{l} = .56$	$\frac{x}{l} = .70$	$\frac{x}{l} = .19$	$\frac{x}{l} = .38$	$\frac{x}{l} = .56$	$\frac{x}{l} = .19$	$\frac{x}{l} = .38$	$\frac{x}{l} = .56$	$\frac{x}{l} = .70$
1761.67	715	704	706	711	735	715	729	699	668	671	686
1761.87	691	687	687	693	719	700	716	700	682	673	673
1762.08	689	682	686	691	704	680	694	700	671	669	682
1762.28	708	695	699	706	730	717	727	695	686	682	690
1762.48	701	692	686	686	721	704	717	692	679	661	690
1762.68	692	674	681	688	714	692	706	701	667	670	672
1762.88	702	695	691	697	726	713	720	688	681	671	677
1763.08	715	697	697	697	728	715	724	690	685	683	697
1763.29	687	677	678	669	697	673	698	698	668	657	673
1763.49	692	679	677	692	716	694	710	663	674	670	670
1763.69	701	689	687	707	737	714	735	701	682	671	678
1763.89	713	704	696	709	726	720	728	720	695	683	694
1764.09	682	671	667	684	710	691	694	688	664	658	664
1764.29	680	678	669	691	709	682	700	691	668	666	664
1764.49	670	661	659	663	690	679	691	676	656	628	645
1764.70	685	673	667	680	707	687	701	689	666	658	669
1764.90	682	668	648	670	682	668	680	680	657	655	659
1765.10	703	690	692	697	721	708	717	685	683	674	681
1765.30	680	673	666	673	697	689	698	693	659	653	666
1765.50	667	666	667	651	693	680	692	691	657	646	658
1765.70	680	668	670	675	705	684	693	659	661	650	661
1765.91	680	671	675	671	700	691	696	691	662	648	660
1766.11	673	668	664	669	693	686	694	686	655	646	664
1766.31	680	667	672	672	693	676	683	682	656	643	656
1766.51	709	702	701	701	726	714	726	683	683	685	692
1766.71	673	669	665	674	695	678	685	680	658	645	658
1766.91	680	662	660	671	698	682	694	680	660	653	662
1767.12	670	661	663	666	692	675	686	648	645	648	650
1767.32	667	658	656	663	692	674	685	678	654	647	651
1767.52	649	647	645	645	676	658	670	669	647	629	641
1767.72	652	651	649	656	685	667	676	667	651	638	654
1767.92	703	689	690	694	722	707	719	670	652	676	674
1768.12	667	669	652	663	689	685	681	671	656	647	656
1768.33	662	655	646	655	677	671	682	675	655	637	653
1768.53	660	653	649	660	680	669	683	673	651	647	649
1768.73	664	669	650	668	682	676	689	676	655	651	657
1768.93	661	656	650	659	674	670	684	674	654	643	650
1769.13	651	658	647	658	678	663	674	660	640	629	645
1769.33	663	660	647	661	671	676	677	662	651	634	652
1769.53	663	654	650	656	676	667	670	660	645	632	643
1769.74	648	646	641	650	668	664	671	659	641	635	646
1769.94	653	658	647	649	671	669	676	664	649	638	638
1770.14	665	654	647	650	678	665	675	662	645	641	636
1770.34	658	651	647	654	682	669	674	651	644	629	640
1770.54	660	653	649	653	673	664	678	653	648	633	642
1770.74	681	679	675	679	700	696	706	694	674	659	664
1770.95	654	641	639	641	672	659	659	659	641	625	641
1771.15	654	652	648	648	670	661	675	663	647	630	641
1771.35	666	664	657	652	680	673	677	668	657	648	646
1771.55	652	643	641	639	663	657	659	656	639	621	637

TABLE IV. - AFTERBODY TEMPERATURES MEASURED ON PROJECT FIRE REENTRY PACKAGE - Continued

Time from launch, sec	Afterbody temperatures, ^{o}R										
	$\phi = 0^{o}$				$\phi = 120^{o}$			$\phi = 240^{o}$			
	$\frac{x}{l} = .19$	$\frac{x}{l} = .38$	$\frac{x}{l} = .56$	$\frac{x}{l} = .70$	$\frac{x}{l} = .19$	$\frac{x}{l} = .38$	$\frac{x}{l} = .56$	$\frac{x}{l} = .19$	$\frac{x}{l} = .38$	$\frac{x}{l} = .56$	$\frac{x}{l} = .70$
1771.75	649	643	638	638	673	654	668	665	640	636	647
1771.95	648	646	639	644	662	655	667	655	644	630	630
1772.16	653	649	642	651	669	665	669	662	649	635	640
1772.36	638	638	630	636	665	652	650	663	636	623	627
1772.56	646	644	635	644	657	653	666	650	635	633	639
1772.76	651	653	644	646	668	660	669	662	642	626	644
1772.96	645	638	636	643	658	656	659	653	633	625	629
1773.16	642	640	631	633	657	651	660	648	635	624	635
1773.37	628	637	635	639	657	655	662	648	644	626	630
1773.57	647	636	632	636	658	649	663	651	629	616	629
1773.77	653	655	645	647	662	660	665	657	642	625	640
1773.97	652	648	650	651	667	663	680	659	639	630	637
1774.17	654	658	651	649	669	663	674	660	647	629	642
1774.37	642	640	635	638	662	649	665	642	633	620	629
1774.57	645	655	649	645	660	656	670	651	635	627	642
1774.78	673	671	676	670	684	682	692	686	660	650	665
1774.98	635	635	635	637	651	649	651	640	626	611	626
1775.18	642	635	635	635	653	649	658	653	635	622	633
1775.38	642	637	644	637	655	653	664	651	630	626	630
1775.58	628	634	639	634	652	648	651	636	623	608	623
1775.78	651	648	648	650	667	660	669	623	644	637	644
1775.99	673	665	661	661	675	676	679	667	658	647	656
1776.19	633	626	622	626	644	640	647	635	626	613	617
1776.39	631	629	617	631	649	642	647	606	620	609	620
1776.59	636	636	624	631	652	636	654	640	634	610	629
1776.79	630	632	628	632	649	650	664	636	632	614	625
1776.99	657	660	645	653	670	664	678	666	655	633	653
1777.19	653	664	664	662	681	679	687	638	653	647	653
1777.40	630	646	635	633	655	650	664	641	635	617	626
1777.60	632	628	623	623	643	637	646	637	625	608	623
1777.80	631	629	624	627	645	645	656	633	624	618	620
1778.00	626	623	619	619	639	641	649	632	619	606	617
1778.20	636	633	629	625	651	653	663	638	624	609	625
1778.40	631	631	620	629	642	643	649	636	627	613	624
1778.61	633	633	630	628	648	642	655	635	635	615	622
1778.81	617	622	615	613	633	631	640	624	613	595	608
1779.01	632	625	623	625	641	643	645	630	623	609	618
1779.21	616	621	616	614	627	625	637	632	618	599	612
1779.41	632	630	616	621	638	645	652	640	627	612	614
1779.61	659	655	650	653	670	670	678	668	650	637	653
1779.81	623	619	621	621	632	630	646	628	621	603	610
1780.02	631	631	623	625	651	640	657	636	627	609	612
1780.22	630	630	621	624	641	637	646	635	623	606	619
1780.42	623	620	616	618	634	634	645	627	615	598	613
1780.62	630	630	619	628	637	632	646	626	621	608	617
1780.82	623	618	610	614	631	632	637	627	616	596	612
1781.02	625	625	620	622	637	634	640	632	620	609	622
1781.23	621	628	616	614	628	634	637	630	623	603	609
1781.43	623	628	618	621	637	637	648	632	621	600	609
1781.63	610	609	602	604	621	623	630	623	614	598	609

TABLE IV. - AFTERBODY TEMPERATURES MEASURED ON PROJECT FIRE REENTRY PACKAGE - Concluded

Time from launch, sec	Afterbody temperatures, ^{o}R										
	$\phi = 0^{o}$				$\phi = 120^{o}$			$\phi = 240^{o}$			
	$\frac{x}{l} = .19$	$\frac{x}{l} = .38$	$\frac{x}{l} = .56$	$\frac{x}{l} = .70$	$\frac{x}{l} = .19$	$\frac{x}{l} = .38$	$\frac{x}{l} = .56$	$\frac{x}{l} = .19$	$\frac{x}{l} = .38$	$\frac{x}{l} = .56$	$\frac{x}{l} = .70$
1781.83	617	626	613	611	631	637	642	626	615	602	611
1782.03	618	625	618	611	634	632	638	632	622	598	611
1782.23	655	657	653	659	674	670	678	659	657	635	648
1782.43	644	651	651	643	660	653	670	646	642	627	642
1782.64	617	619	613	613	628	631	636	624	617	602	604
1782.84	620	617	613	617	626	628	631	624	610	599	608
1783.04	640	645	633	633	651	645	663	631	642	615	627
1783.24	620	620	609	611	627	624	636	611	615	591	602
1783.44	630	628	616	620	637	637	648	598	623	600	616
1783.64	612	612	606	612	625	623	624	621	610	588	603
1783.85	618	618	609	611	627	625	636	625	616	591	607
1784.05	625	622	615	615	633	634	638	618	615	600	615
1784.25	612	610	606	610	618	621	635	612	607	588	597
1784.45	612	616	607	607	618	612	628	614	609	592	601
1784.65	671	668	664	660	677	675	687	655	648	635	653
1784.85	649	644	647	638	649	651	659	649	633	614	634
1785.06	619	612	610	608	628	622	629	619	606	586	597
1785.26	609	617	611	611	629	622	638	613	611	599	602
1785.46	606	608	599	603	612	617	633	614	612	588	601
1785.66	607	609	605	600	623	625	632	602	607	587	598
1785.86	626	626	616	620	630	633	641	628	626	606	618
1786.06	612	616	616	614	631	630	641	616	616	594	603
1786.27	610	616	594	603	612	623	626	612	605	581	603
1786.47	611	613	604	604	617	622	633	606	606	588	604
1786.67	631	627	623	620	629	629	648	627	629	609	618
1786.87	611	606	602	604	611	615	624	608	604	584	595
1787.07	607	609	603	601	612	612	604	578	603	581	592
1787.27	641	639	640	644	654	655	660	646	634	617	631
1787.47	611	606	615	604	619	615	633	626	610	593	597
1787.67	626	630	635	622	638	645	642	630	625	604	611
1787.87	657	661	655	651	659	666	670	665	642	633	638
1788.07	601	609	603	610	620	620	630	614	594	578	590
1788.27	594	607	612	599	614	621	624	612	598	579	596
1788.48	626	628	629	618	630	670	638	630	624	607	616
1788.68	628	633	642	644	659	660	678	668	653	617	624
1788.88	614	632	607	630	637	625	646	623	776	596	598
1789.08	628	626	635	628	641	637	671	633	637	604	617
1789.28	594	603	605	589	598	603	618	603	598	575	580
1789.49	625	627	619	619	627	628	639	619	621	605	605
1789.69	639	637	628	635	645	639	651	636	630	611	622
1789.90	612	603	599	601	609	612	615	609	609	590	590
1790.10	632	632	630	626	630	628	645	630	628	611	622

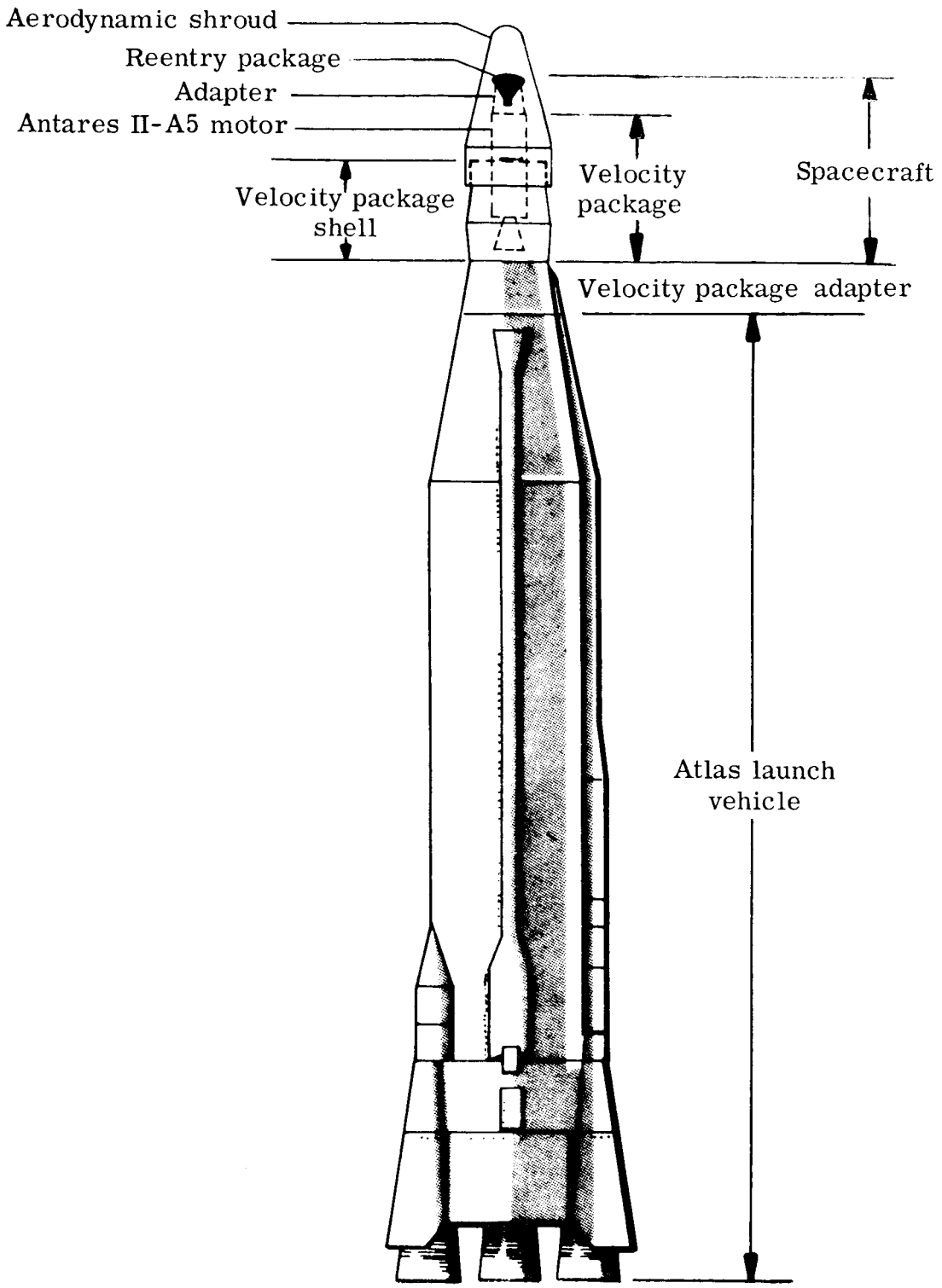

Figure 1.- Schematic drawing of Project Fire space vehicle.

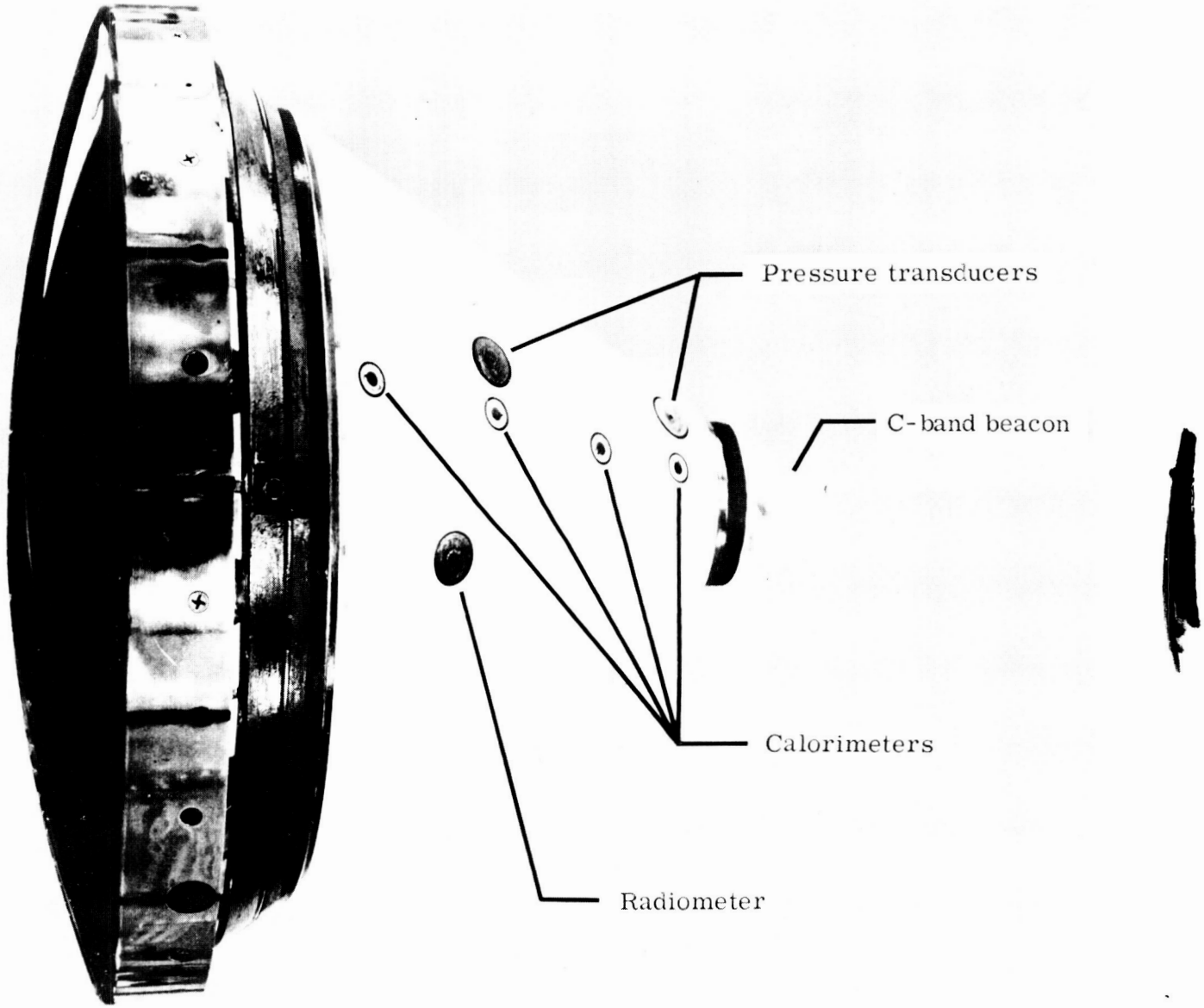

Figure 2.- Photograph of reentry package.

L-65-193

Beryllium heat-shield number	D_m, in.	R_n, in.	R_c, in.
1	26.44	36.80	0.40
2	24.80	31.70	1.40
3	23.11	27.64	.24

Key to afterbody instrumentation

+ - Gold calorimeters
△ - Pressure sensors
○ - Radiometer
▨ - Telemetry antenna
◘ - C-band beacon antenna

NOTE: Dimensional location of afterbody sensors is shown in Table I.

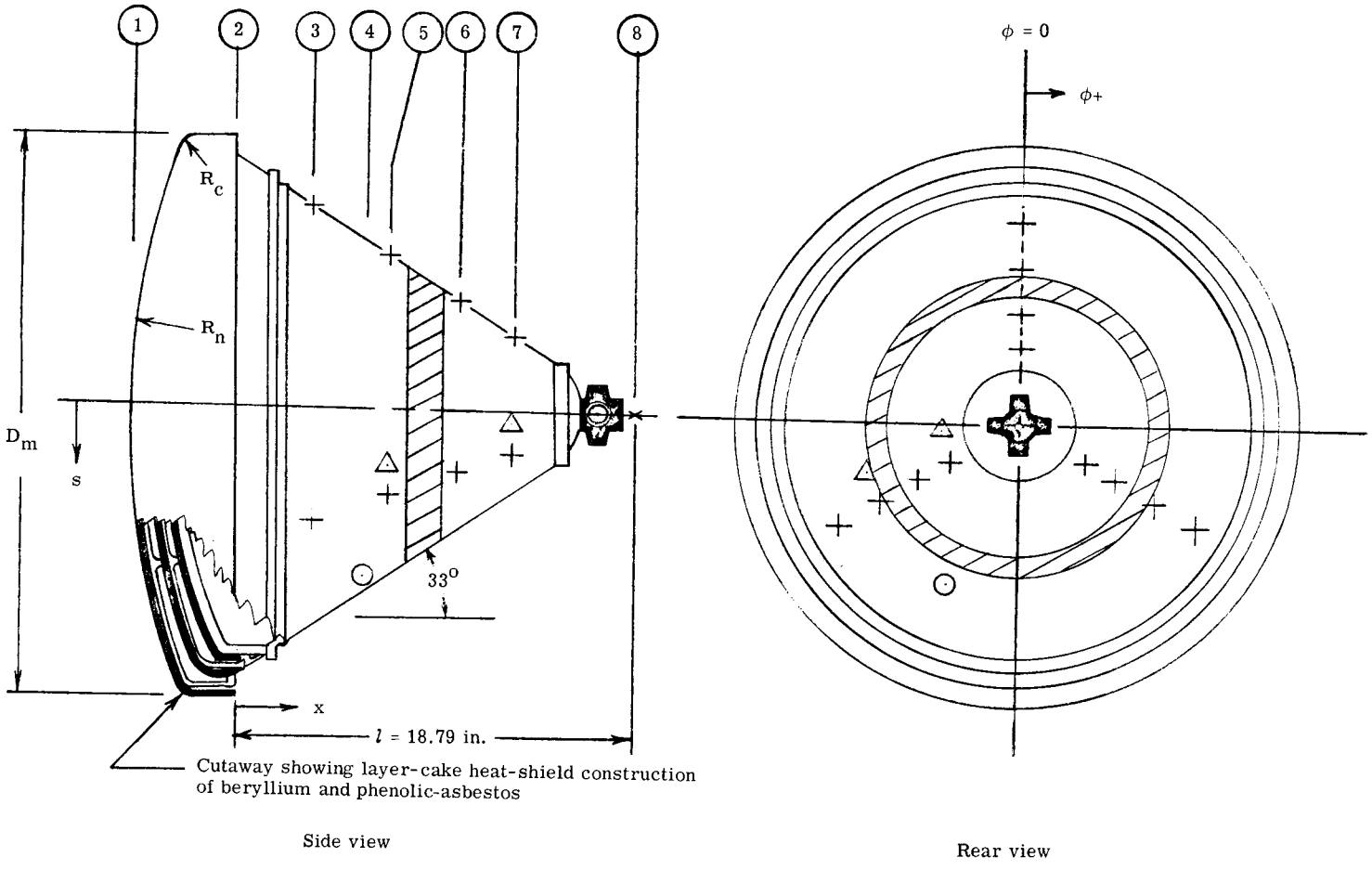

Figure 3.- Reentry package geometry.

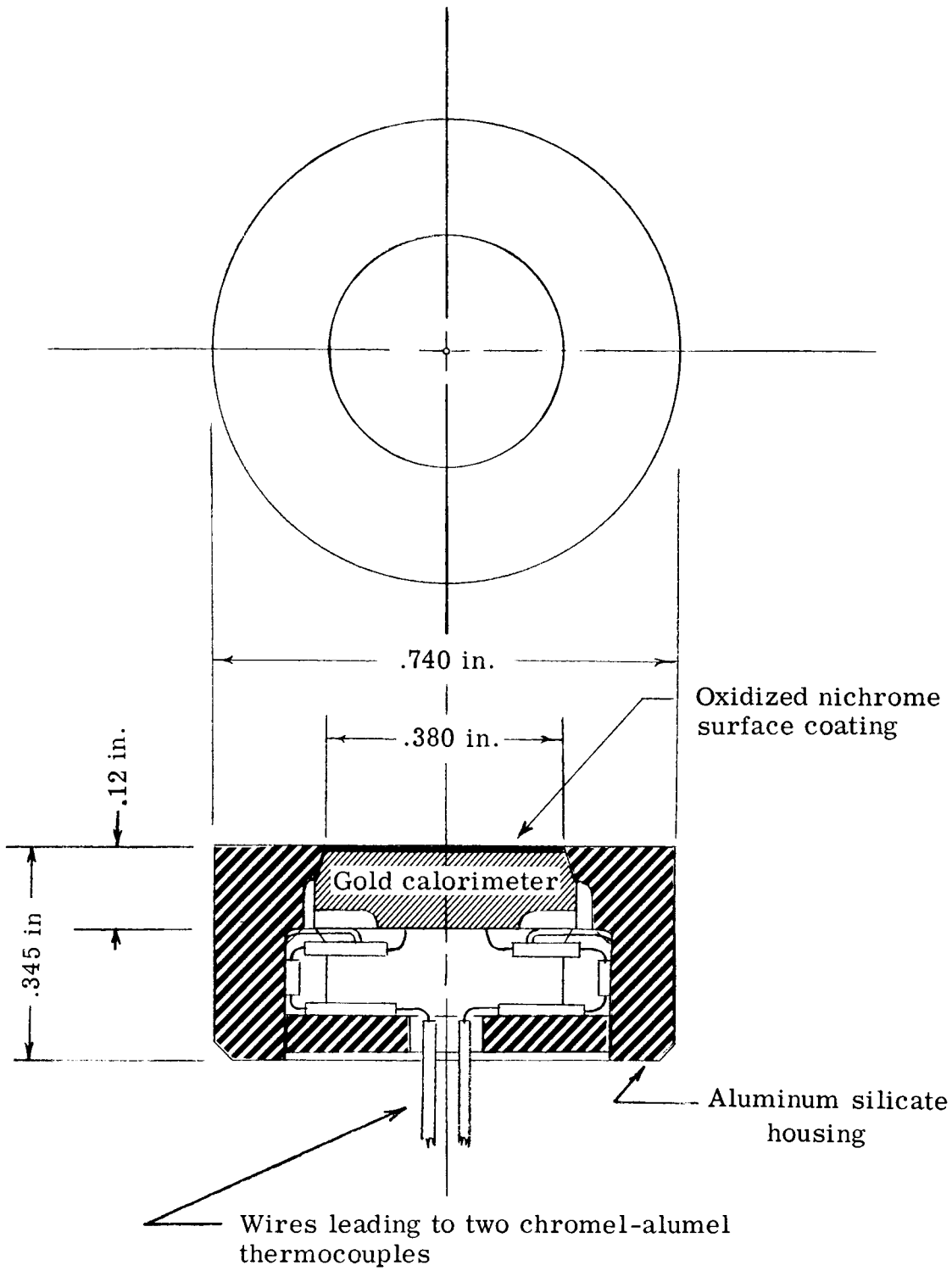

Figure 4.- Schematic drawing of gold calorimeter and insulating housing.

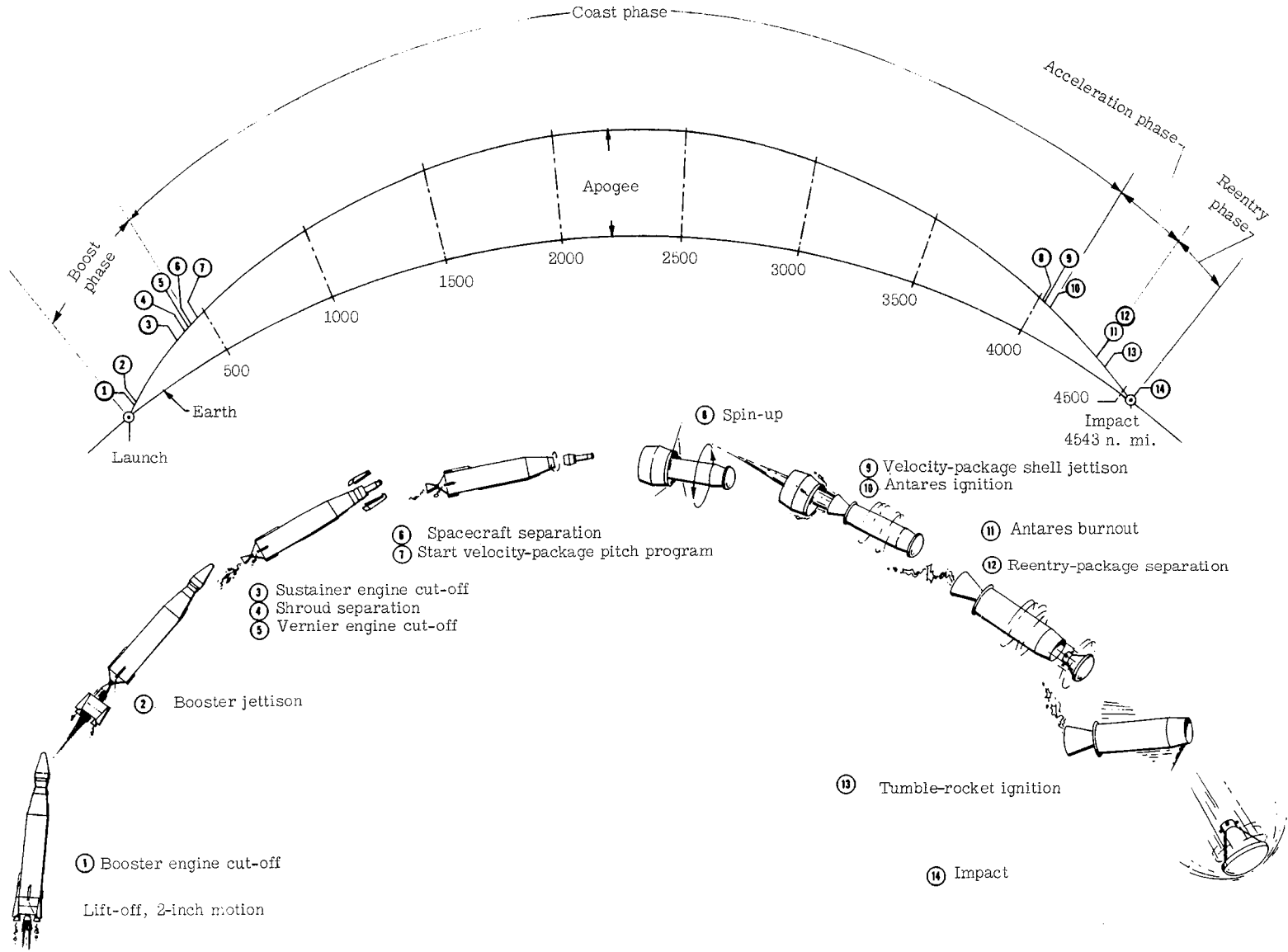

Figure 5.- Project Fire vehicle trajectory and flight sequence of events.

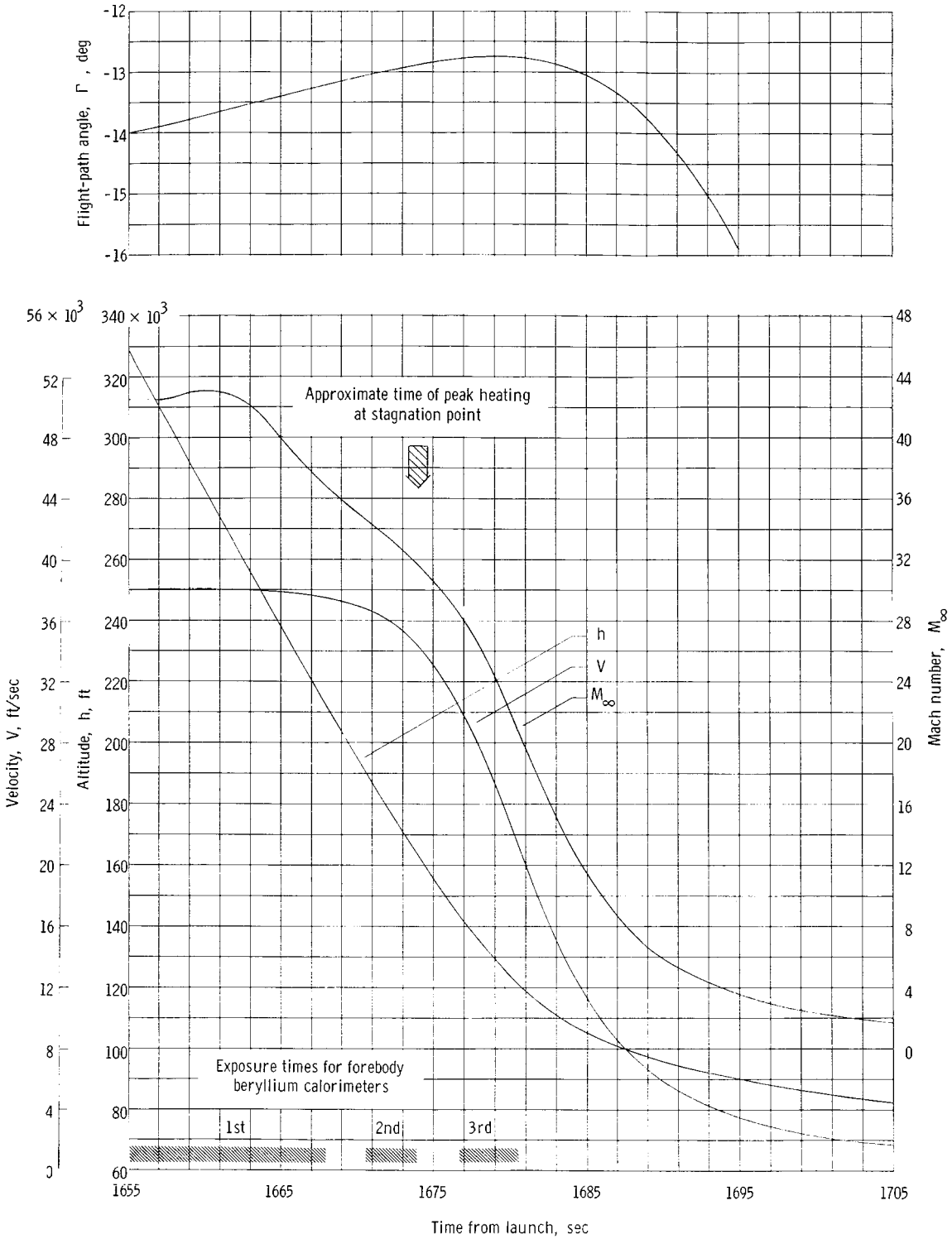

Figure 6.- Reentry trajectory parameters.

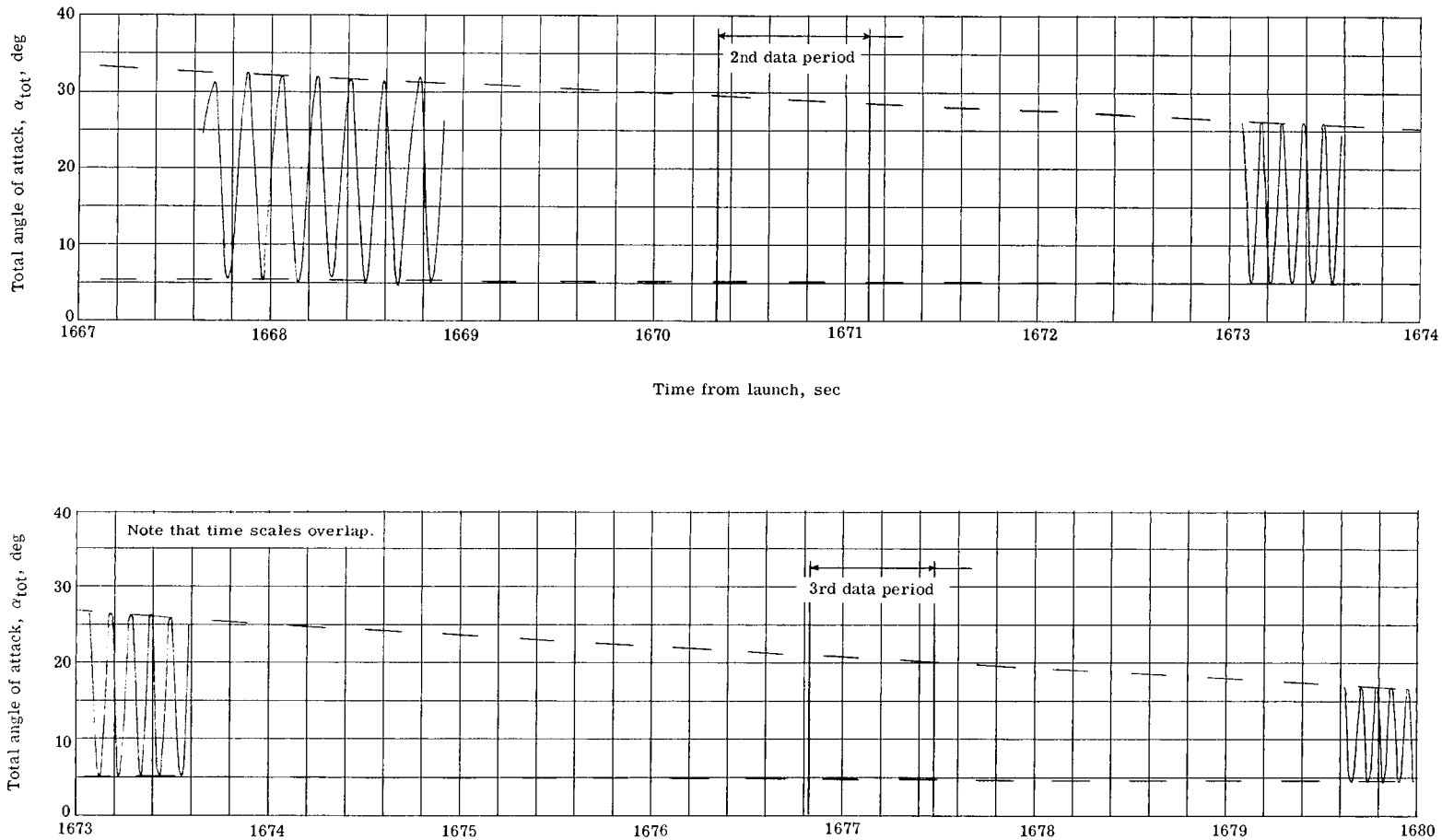

Figure 7.- Calculated total-angle-of-attack history for Fire 1 reentry package.

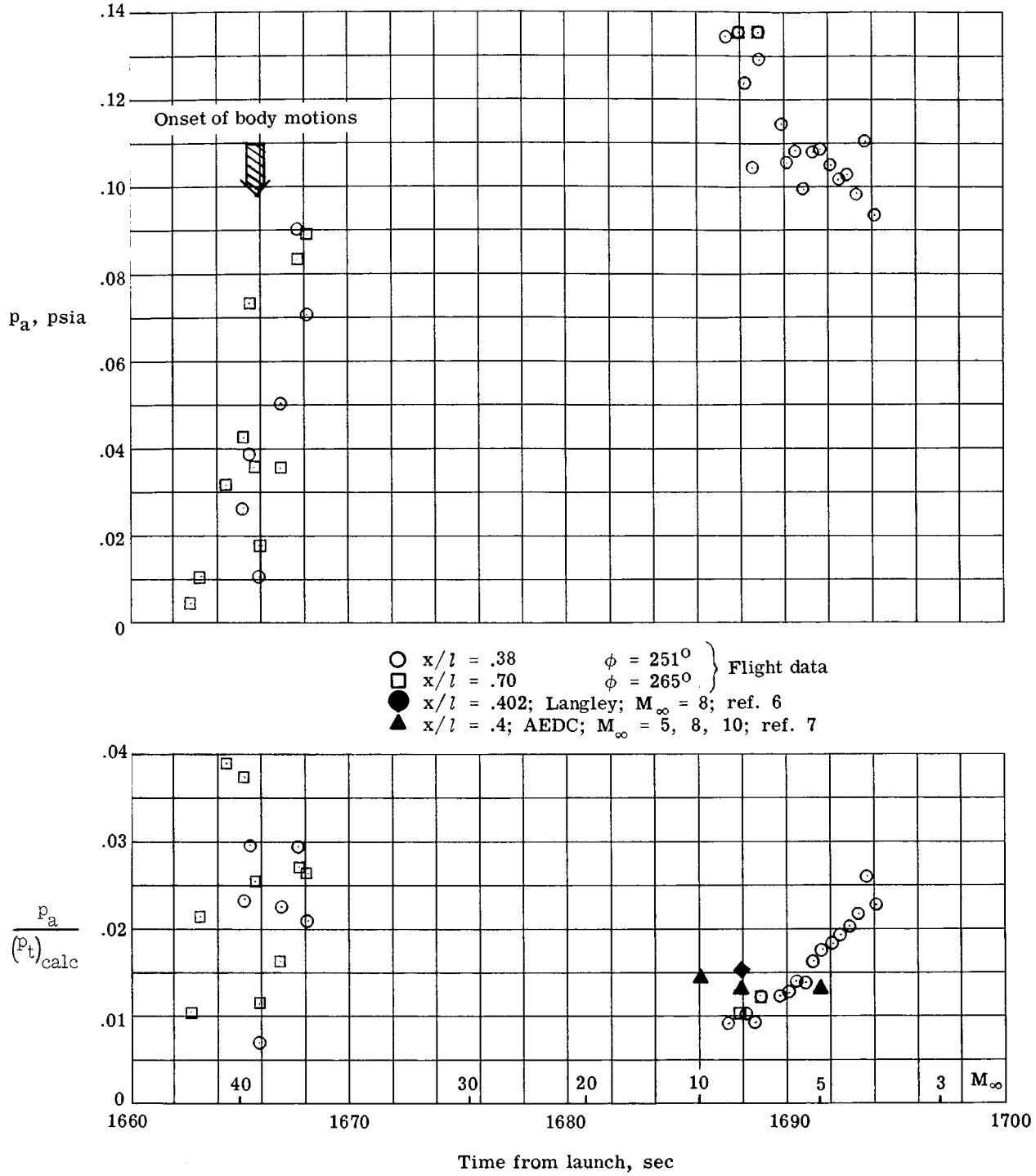

Figure 8.- Afterbody pressures measured during the Fire 1 reentry.

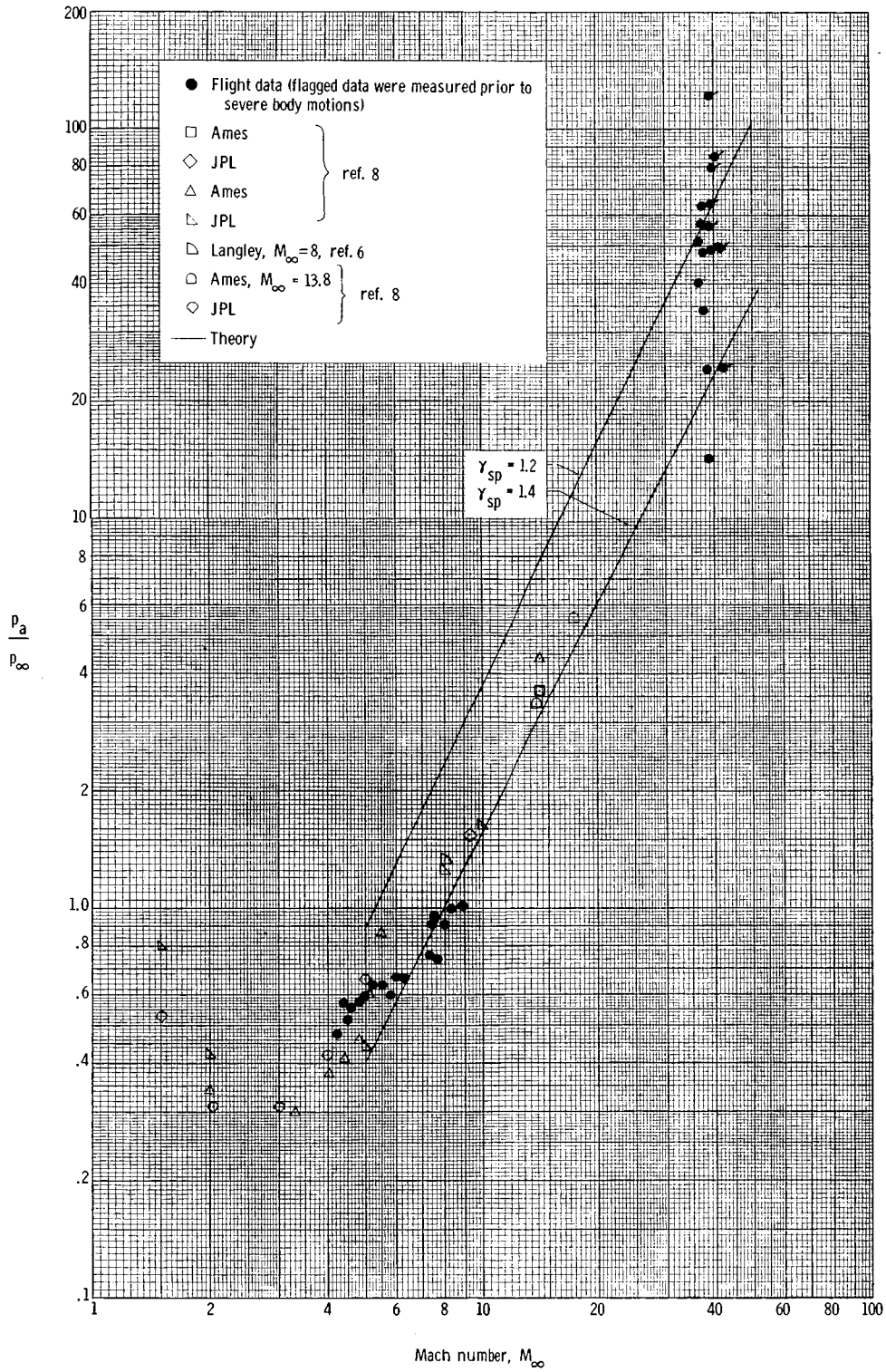

Figure 9.- Correlation of flight and wind-tunnel measurements of afterbody pressures on Apollo-shaped bodies.

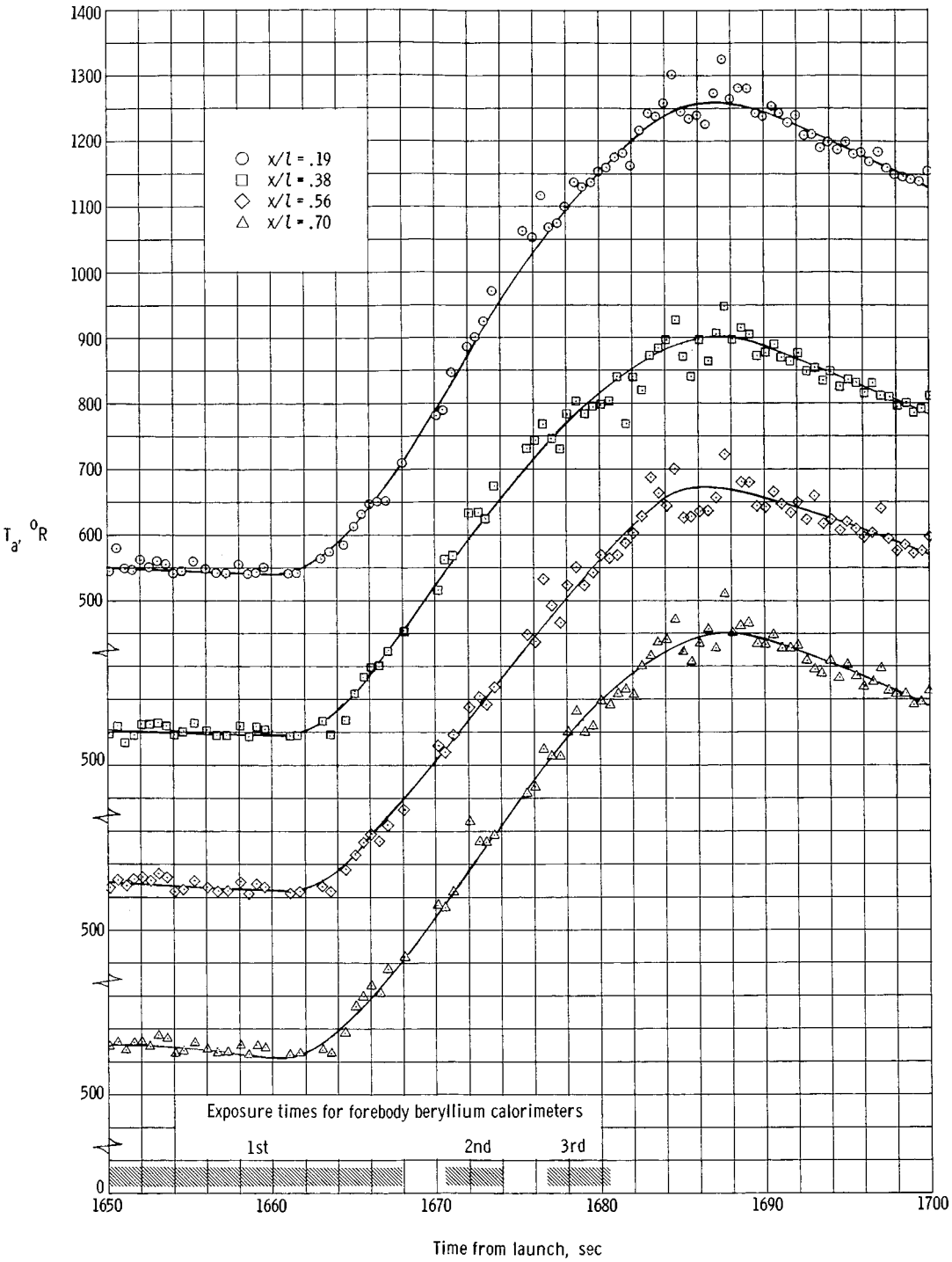

(a) $\phi = 0^0$.

Figure 10.- The variation of afterbody temperature with time from launch.

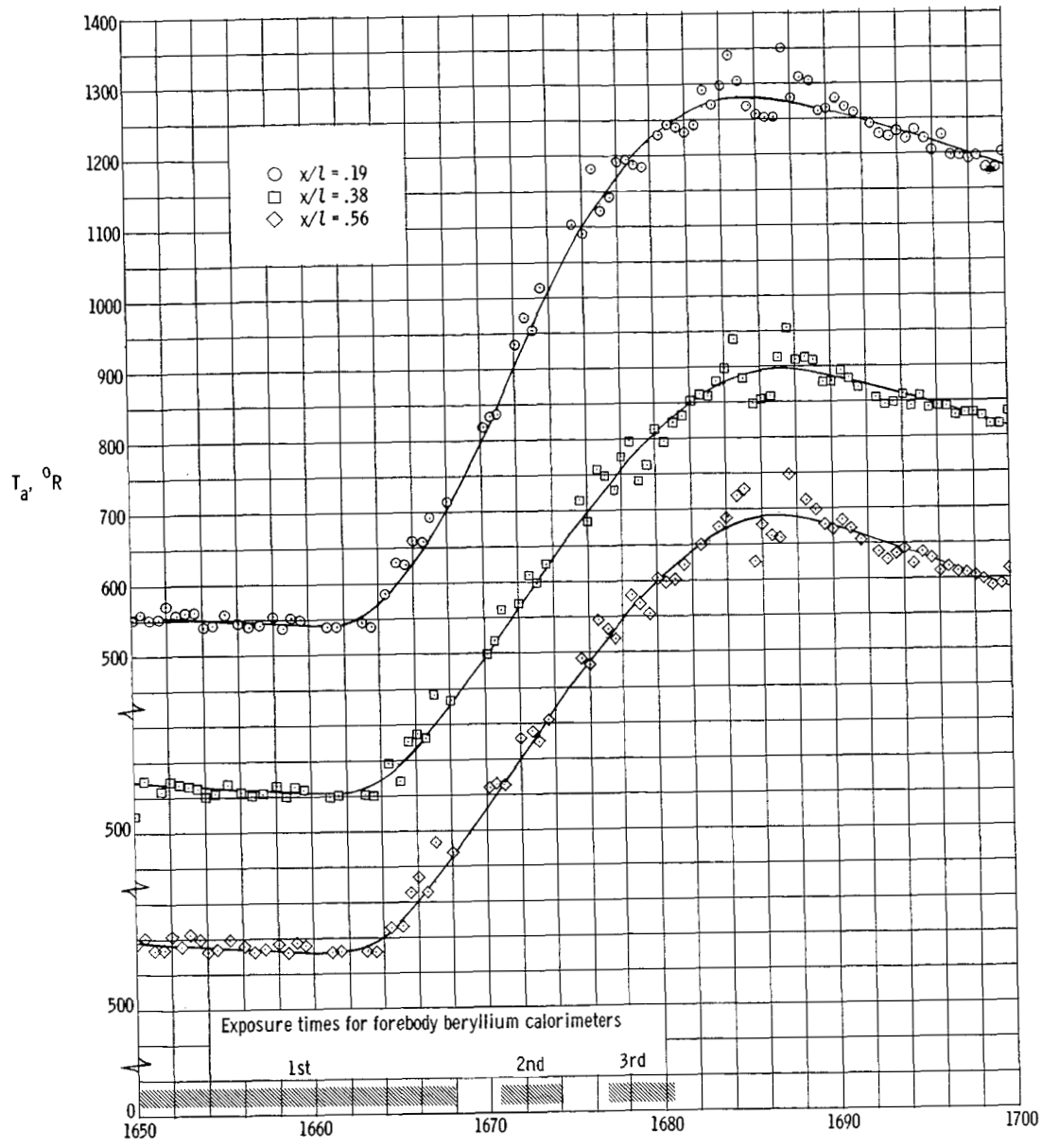

(b) $\emptyset = 120^0$.

Figure 10.- Continued.

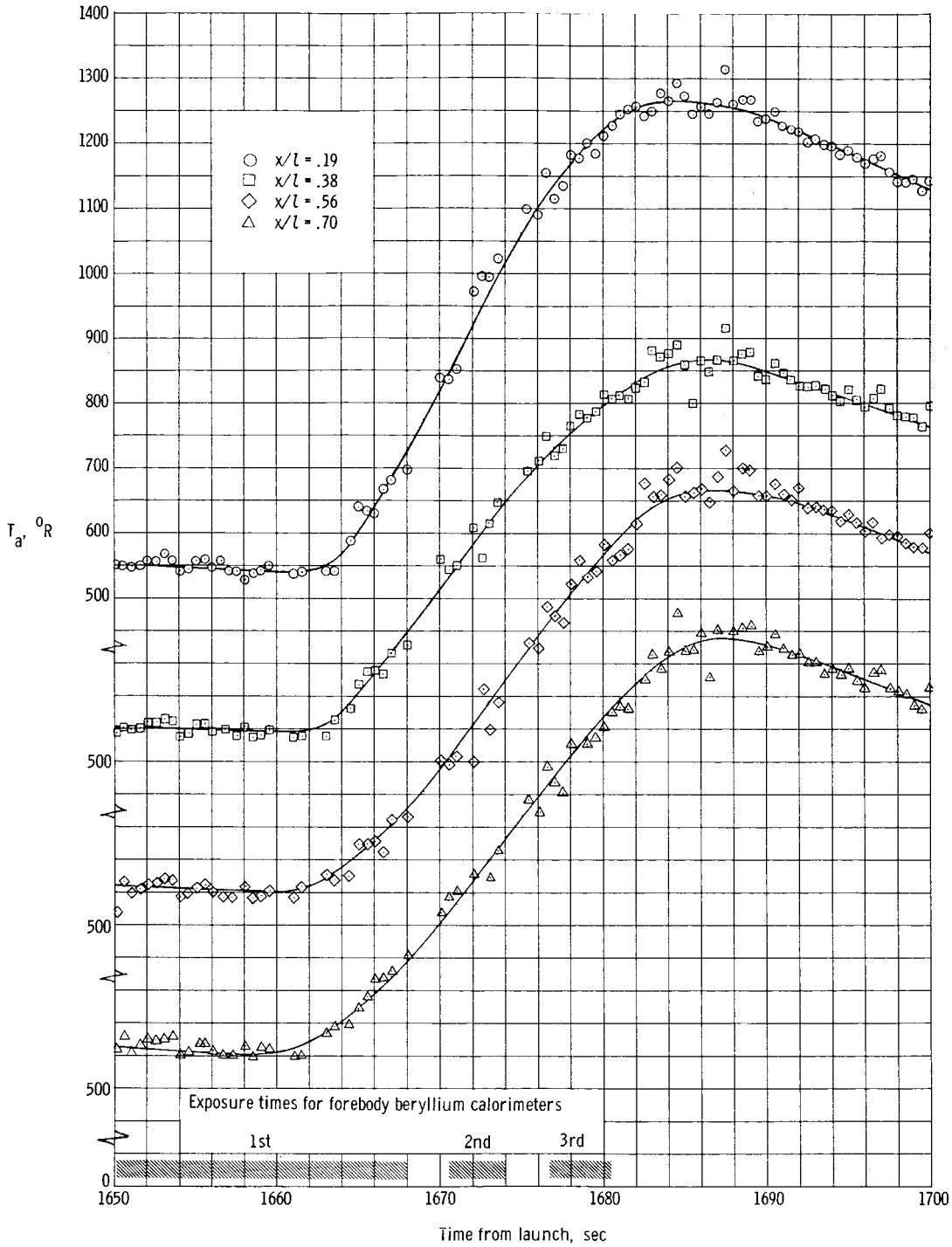

(c) $\phi = 240^o$.

Figure 10.- Concluded.

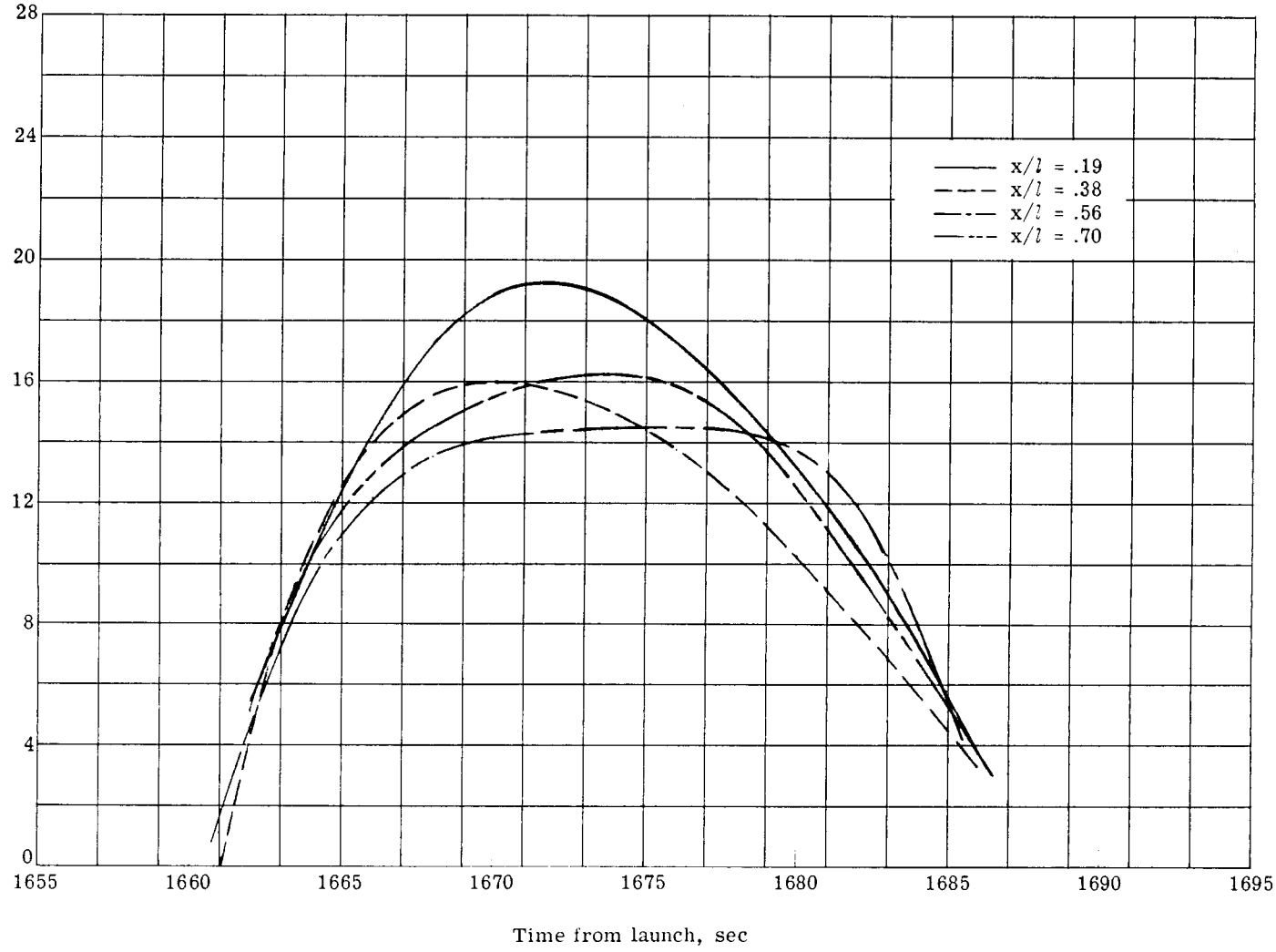

(a) $\phi = 0^0$.

Figure 11.- The variation of afterbody heating rates with time from launch.

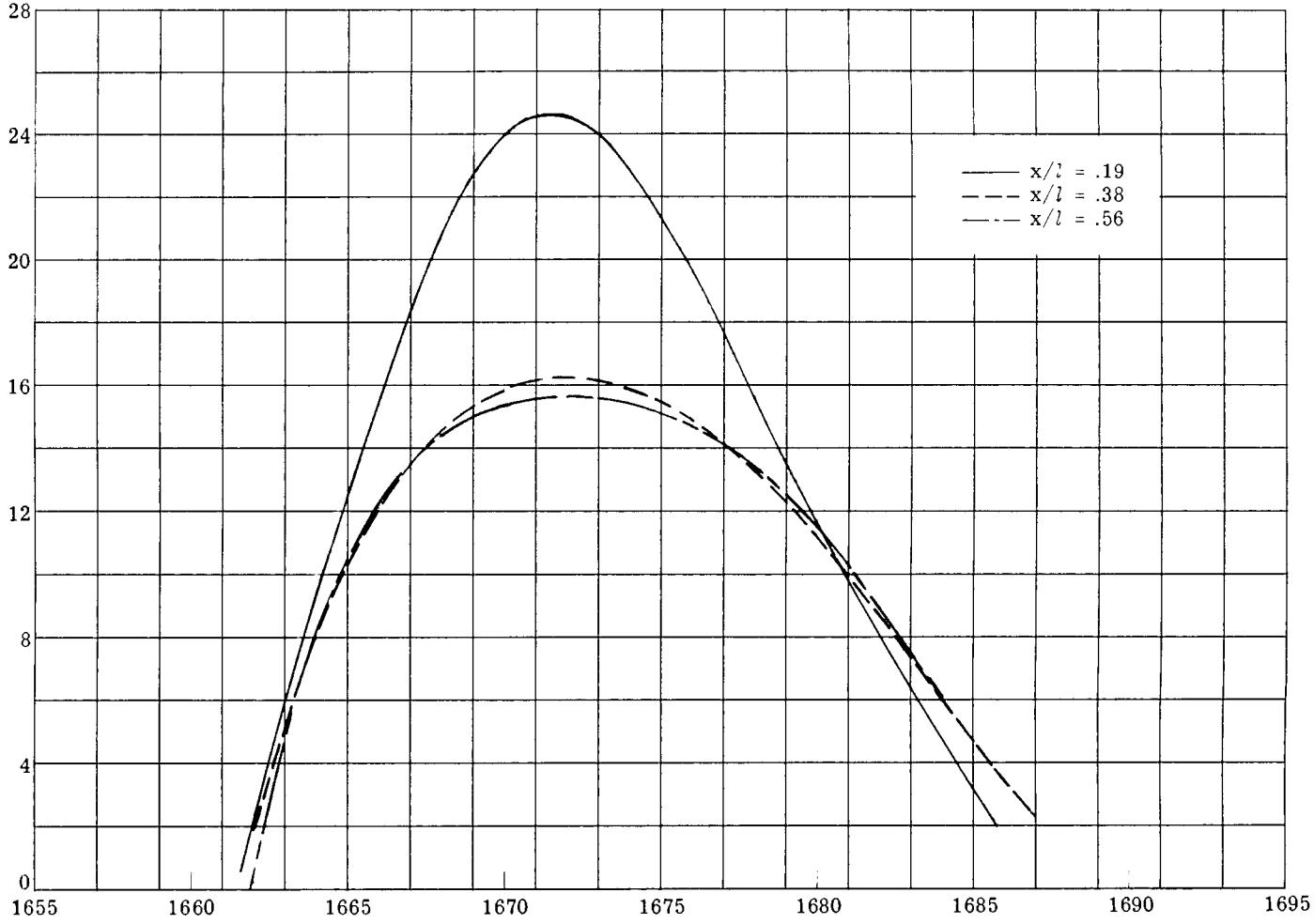

(b) $\phi = 120^0$.

Figure 11.- Continued.

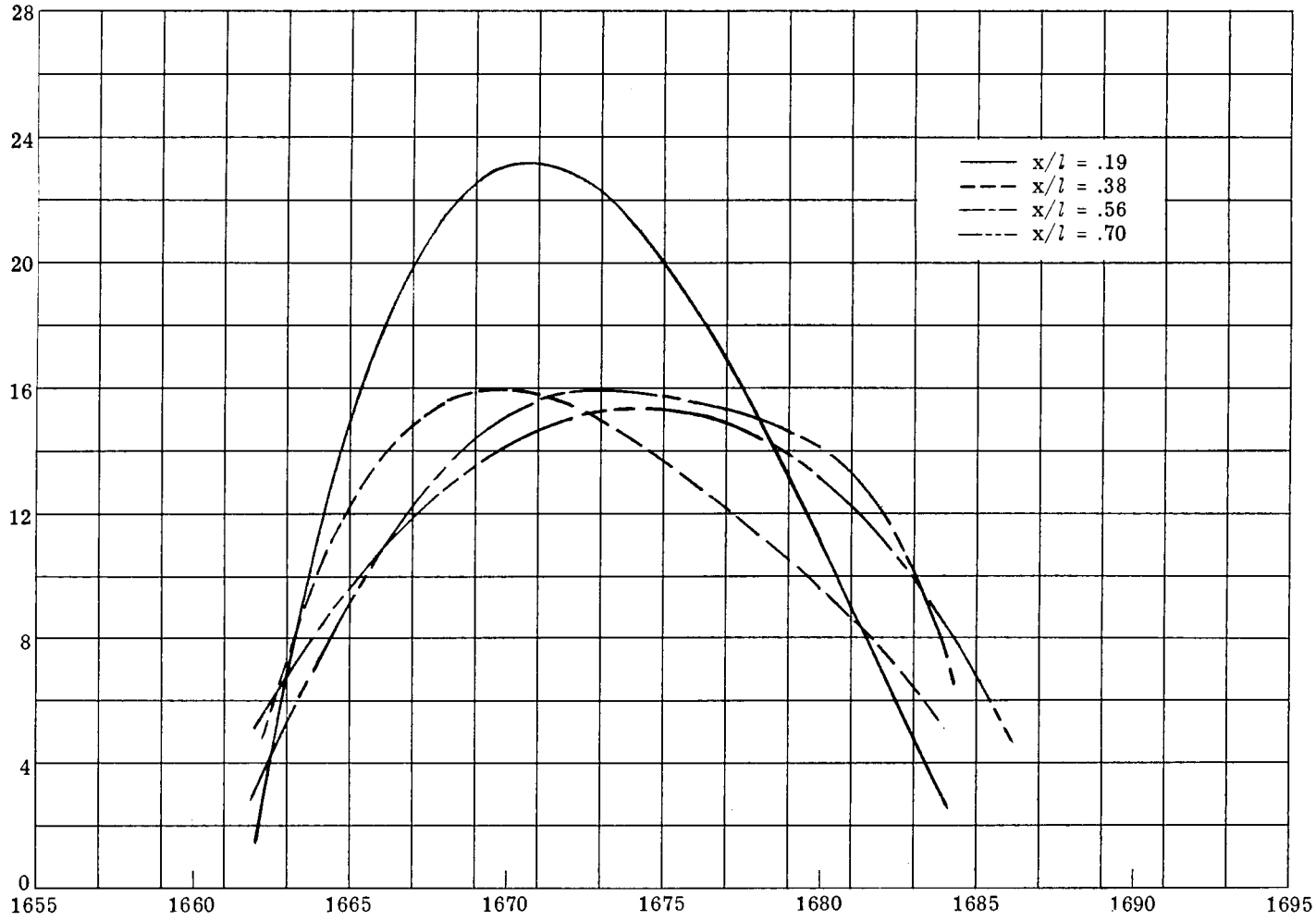

(c) $\phi = 240^0$.

Figure 11.- Concluded.

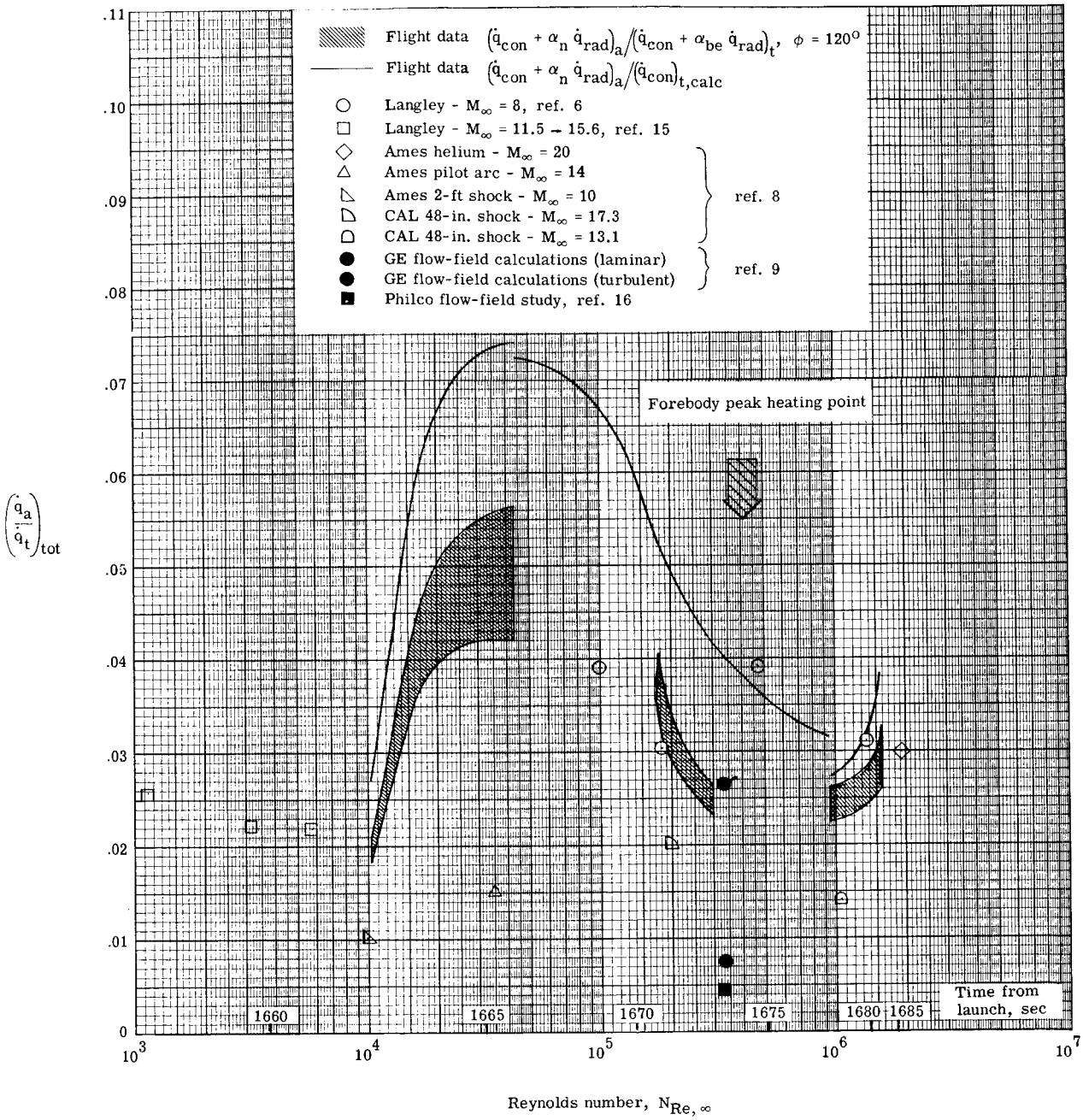

Figure 12.- Comparison of afterbody heating rates measured in flight with wind-tunnel data and theoretical calculations for $x/l = 0.19$.

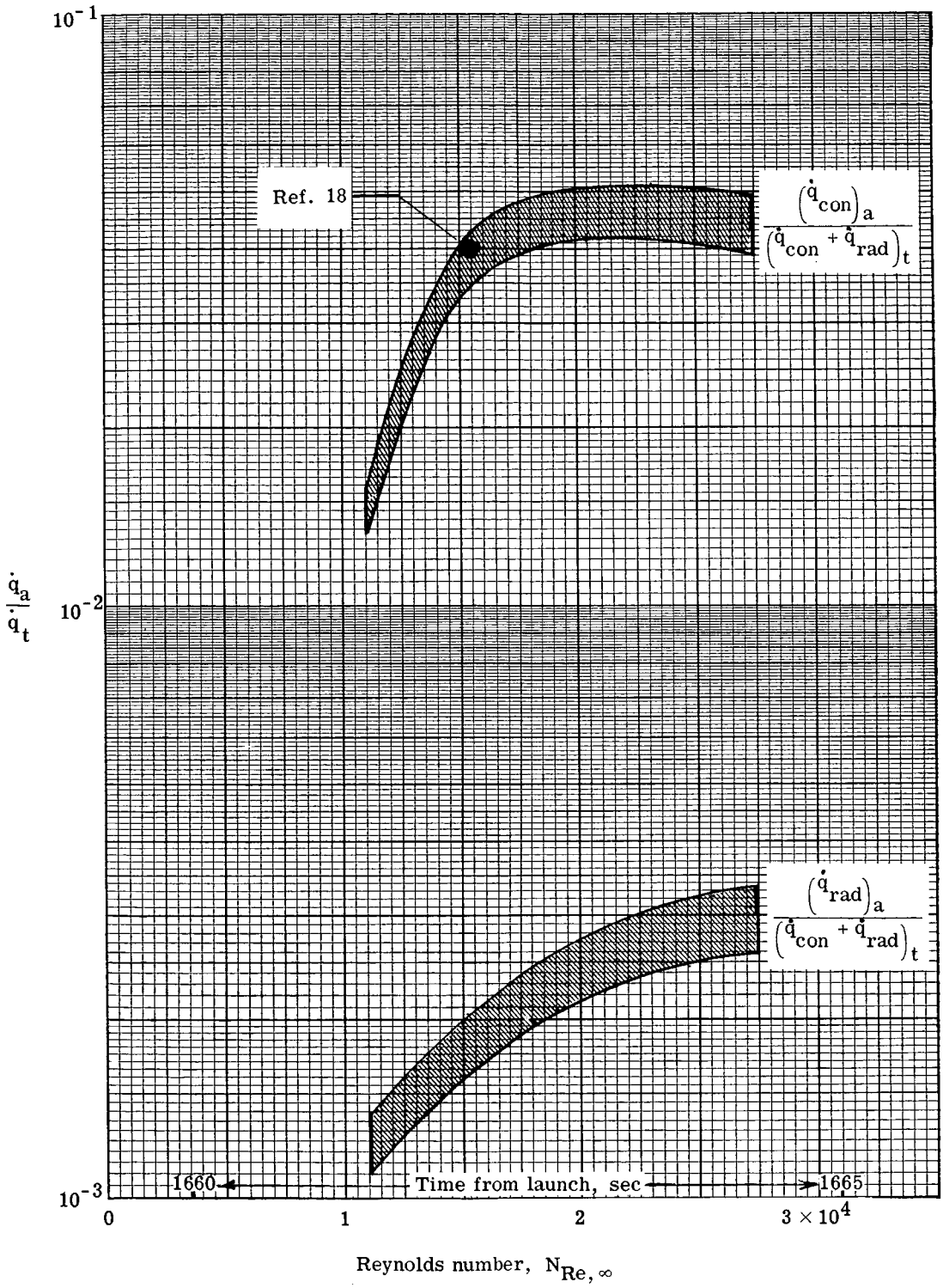

Figure 13.- Separated convective and radiative heating rates on the reentry-package afterbody early in flight. $x/l = 0.38$; $\phi = 240^0$.